National Défense
Defence nationale

ADAPTIVE SUPPRESSION OF INTERFERENCE IN HF SURFACE WAVE RADAR USING AUXILIARY HORIZONTAL DIPOLE ANTENNAS

by

Hank W.H. Leong

DEFENCE RESEARCH ESTABLISHMENT OTTAWA
REPORT NO. 1336

Canada

September 1998
Ottawa

National Defence / Défense nationale

ADAPTIVE SUPPRESSION OF INTERFERENCE IN HF SURFACE WAVE RADAR USING AUXILIARY HORIZONTAL DIPOLE ANTENNAS

by

Hank W.H. Leong
Ground Based Radar Group
Surface Radar Section

DEFENCE RESEARCH ESTABLISHMENT OTTAWA
REPORT NO. 1336

PROJECT
05AB11

September 1998
Ottawa

Adaptive Suppression of Interference in HF Surface Wave Radar Using Auxiliary Horizontal Dipole Antennas

Abstract

This report presents the results of a study to evaluate the effectiveness of an adaptive technique using horizontal dipoles to suppress the skywave interference in HF Surface Wave Radar (HFSWR). Four auxiliary horizontal dipole antennas, configured in the form of two separate crosses, were used to form an adaptive system with the vertically polarized antennas (VPA) of a HFSWR system. The outputs of the horizontal dipoles were correlated with the summed output of the VPAs to cancel the interference component in the output of the VPAs. Two slightly different methods were used in the estimation of the correlation coefficients. The first method used the samples at the far ranges of the radar, and the second method used the samples in the range bins close to the range bin selected for the interference suppression. With the first method, the interference-plus-noise power (INP) was reduced by up to 13 dB, and the Bragg-to-interference-plus-noise-ratio (BINR) was increased by up to 21 dB. With the second method, the INP was reduced by up to 17 dB, and the BINR was increased by up to 25 dB. In both methods, we compared the effectiveness of the adaptive technique using one, two or four horizontal dipole antennas. As expected, we found the technique to be most effective when all four horizontal dipoles were used.

Suppression adaptable de l'interférence des radars à onde de surface décamétrique au moyen d'antennes auxiliaires de dipôles horizontaux

Résumé

Voici les résultats d'une étude ayant servi à évaluer l'efficacité de la technique adaptable utilisant des dipôles horizontaux pour supprimer l'interférence des ondes ionosphériques dans les radars à onde de surface décamétrique (HFSWR). Quatre antennes auxiliaires de dipôle horizontaux, disposées selon deux croix séparées, ont servi à former un système adaptable avec les antennes polarisées verticalement du système HFSWR. On a mis en corrélation les sorties des dipôles horizontaux et des antennes polarisées verticalement afin de supprimer l'interference. Deux méthodes légèrement différentes ont etë utilisëes pour évaluer les coefficients de corrélation. La première méthode a utilisëe les donnëes radar pour les grandes distances, et la seconde a utilisëe les donnëes radar pour des distances proches de celle sélectionnée pour la suppression de l'interfërence. La première méthode a permis de réduire de 13 dB la puissance de l'interférence et du bruit (INP) et d'accroître de 21 dB le rapport Bragg sur interférence plus bruit (BINR). Quant à la seconde, elle a permis de réduire l'INP de 17 dB, et le BINR de 25 dB. Dans les deux méthodes, on a comparëes l'efficacité de la technique adaptable à l'aide de une, deux ou quatre antennes de dipôles horizontaux. Comme prévu, cette technique est plus efficace lorsqu'on emploie quatre dipôles horizontaux.

Executive Summary

A coastal surveillance HF Surface Wave Radar (HFSWR) is capable of detecting ship and aircraft targets beyond the line of sight at distances up to 500 km. The radar is usually operated in the frequency band of 2-15 MHz. One problem encountered in the operation of the radar is that of nighttime skywave interference. Ionospheric conditions at night favour the propagation of these radio signals over very long distances. This effectively increases the number of interfering signals in the above frequency band at a given radar site, making it sometimes impossible to find a clear channel to operate the radar.

The interfering signals contaminate the data in the HFSWR and reduce the target signal-to-interference-plus-noise ratio (SINR) in the data. The target signals are vertically polarized, and the interfering signals are elliptically polarized [1] or partially polarized [2]. One approach to alleviate this interference problem is to utilize the difference of the polarization characteristics. Horizontally polarized antennas (HPA) can be added to a HFSWR system that uses vertically polarized antennas (VPA). The interfering signals received by the VPAs correlate with those received by the HPAs. From this correlation, we can use the outputs of the HPAs to estimate the interference component at the output of the VPAs. A subtraction of this estimate from the output of the VPAs would then result in an increase of the target SINR in the radar data.

A radar experiment was carried out to study the effectiveness of this technique. Four horizontal dipole antennas, configured as two separate crosses, were used as auxiliary antennas in a HFSWR to receive data during nighttime hours when the interference was the strongest. A variant of the sample matrix inversion (SMI) method [4] was implemented to estimate and cancel the interference component. In normal operations, the outputs of the VPAs in the HFSWR are combined in a specified manner to produce a 'main antenna' output in a specified look direction. The SMI-based algorithm used the correlation between the outputs of the main and auxiliary antennas to

estimate weights for the auxiliary antenna outputs. The weighted outputs of the auxiliary antennas were summed, and the sum was treated as an estimate of the interference and then subtracted from the output of the main channel. Two slightly different methods of implementation were studied. The first method used the echoes at the far ranges of the radar, and the second method used the echoes in ranges close to the range selected for interference suppression.

The results show that both methods worked well against the observed nighttime skywave interference. The performance of the adaptive technique is measured by the amount of interference (plus noise) that is removed from the main channel output and by the amount of target signal that is enhanced after the interference suppression. The radar signal includes the first-order and second-order sea echoes, and the first-order sea echo is referred to as Bragg lines [8]. Since no target signals could be observed from the radar data, we used the Bragg lines as performance indicators. With the first implementation method, the interference-plus-noise power (INP) was reduced by up to 13 dB, and the Bragg-to-interference-plus-noise-ratio (BINR) was increased by up to 21 dB. With the second method, the INP was reduced by up to 17 dB, and the BINR was increased by up to 25 dB. In both methods, we also compared the effectiveness of the adaptive technique using one, two or four horizontal dipole antennas. As expected, we found the technique to be most effective when all four horizontal dipoles were used.

Table of Contents

List of Figures

List of Tables

1. Introduction

A high-frequency surface-wave radar (HFSWR) utilizes the surface-wave mode of electromagnetic wave propagation over sea water to detect targets (e.g., ships and aircraft) at distances beyond the line of sight. The radar is ideally suited as a cost-effective sensor for wide-area surveillance of coastal waters at distances up to 500 km. For ship and aircraft detection, the HFSWR is usually operated in the frequency band of 2-15 MHz. One problem encountered in the operation of the radar in this frequency band is that of night-time interference propagated via the skywave mode from other users of the same frequency band. Ionospheric conditions at night favour the propagation of radio signals over very long distances. This effectively increases the number of interfering signals in the frequency band at a given radar site, making it sometimes impossible to find a clear channel to operate the radar.

The skywave-propagated signal is elliptically polarized [1] or partially polarized [2], and the desired HFSWR signal is vertically polarized. One approach to alleviate the interference problem is to utilize the difference of the polarization characteristics. Auxiliary horizontally polarized antennas (HPA) can be used to form an adaptive system with the vertically polarized antennas (VPA) that are used in the HFSWR. The horizontally polarized signals received by the HPAs correlate with the interfering signals received by the VPAs. From this correlation, we can estimate the interference components in the outputs of the VPAs. A subtraction of the estimates from the outputs of the VPAs can then result in a suppression of the interference in the radar data.

The ionosphere is time-variant and dispersive in nature, and the polarization of the interfering signal changes with time and frequency. Hence, the system that employs the HPAs must be adaptive. Madden [3] has investigated the feasibility of using this adaptive technique in a practical HFSWR system. Promising results were reported from a HFSWR that included one auxiliary horizontal dipole antenna. We have carried out a similar radar experiment to study the effectiveness

of this adaptive technique using multiple horizontal dipole antennas. Four horizontal dipoles, configured in the form of two separate crosses, were used as auxiliary antennas in a HFSWR located at Cape Race, Newfoundland. Six VPAs of a forty-element array were also used in the experiment. Figure 1 shows a top view of the antenna configuration.

A variant of the sample matrix inversion (SMI) method [4] was implemented to estimate and cancel the interference component in the summed output of the VPAs. This SMI-based algorithm uses the correlation between the outputs of the vertical and horizontal antennas to estimate weights for the outputs of the auxiliary horizontal antennas. Two slightly different methods were used to estimate and update these weights. The first method used the echoes at the far ranges of the radar. The second method used the echoes in ranges close to the range selected for interference suppression. In this report, we present the results of using these two methods in conjunction with many different combinations of the auxiliary horizontal dipole antennas to study the effectiveness of the adaptive technique.

The organization of this report is as follows. Section 2 provides a detailed description of the radar experiment. Section 3 presents the results of a preliminary analysis of the data from the experiment. In Section 4, we describe the adaptive system and the adaptive algorithms. In Section 5, we describe the Doppler processing procedure used for the radar data. Section 6 contains the results of the study using the two methods to suppress the interference. Finally, Section 7 gives the conclusions and recommendation.

2. The Radar Experiment

As shown in Figure 1, the four auxiliary horizontal dipole antennas (Elements 1-4) were configured as two separate crosses and were located behind the vertical receive array of the HFSWR. The vertical array was aligned with the coastline at Cape Race. It was linear, uniform, and consisted

of 40 vertical monopoles spaced at a distance of 22.2 m (i.e., one half of a wavelength at the design radar frequency of 6.75 MHz). Ten receivers were available. Four were connected to the auxiliary horizontal dipole antennas, and the other six were connected to the central six vertical monopoles (Elements 18-23 in the array, re-numbered, respectively, as Elements 5-10 in the experiments). Table I shows the connections of the receivers to the different antennas.

Table I Connections of Receivers to Different Antenna Elements

Receiver No.	Antenna Type	Remarks
1	Horizontal Dipole	Perpendicular to Vertical Array
2	Horizontal Dipole	Parallel to Vertical Array
3	Horizontal Dipole	Parallel to Vertical Array
4	Horizontal Dipole	Perpendicular to Vertical Array
5	Vertical Monopole	Element #18
6	Vertical Monopole	Element #19
7	Vertical Monopole	Element #20
8	Vertical Monopole	Element #21
9	Vertical Monopole	Element #22
10	Vertical Monopole	Element #23

The experiment was carried out during nighttime, when the interference was the strongest. Data collection started at 02:22:44 AM and finished at 03:10:05 AM, local time, on 29 March 1995. The radar used a frequency-modulated interrupted continuous waveform (FMICW) [5] in the experiment. The FMICW radar was operated at a nominal frequency of 5.811 MHz with a swept bandwidth of 125 kHz and a waveform repetition frequency (WRF) of 9.01 Hz. The radar had a waveform repetition interval (WRI) of 110 milli-seconds. In each WRI, each of the radar receivers sampled echoes returned from 256 consecutive range bins. The range resolution of the radar was

1.2 km, and the first range bin of the radar was centred at 2 km. Hence, the echoes were returned from ranges between 2 and 308 km.

3. Preliminary Data Analysis

The 10-element array received radar echoes continuously for about 47 minutes. Table II shows the covariance matrix of the array in terms of magnitude (r_{ij}) and phase (θ_{ij}), constructed from all the outputs of the array elements. The 10x10 covariance matrix, denoted by **C**, can be divided into four submatrices:

(1) The 4x4 submatrix, $\mathbf{C}_1$, on the upper left corner of the main matrix;
(2) The 6x6 submatrix, $\mathbf{C}_2$, on the lower right corner of the main matrix;
(3) The 4x6 submatrix, $\mathbf{C}_3$, on the upper right corner of the main matrix;
(4) The 6x4 submatrix, $\mathbf{C}_4$, on the lower left corner of the main matrix.

Submatrix $\mathbf{C}_1$ represents the covariance matrix of the four horizontal dipole antennas. $\mathbf{C}_2$ represents the covariance matrix of the six vertically polarized antennas. In $\mathbf{C}_3$ are the cross-correlation coefficients between the horizontal dipole antennas and the VPAs, and in $\mathbf{C}_4$ are the cross-correlation coefficients between the VPAs and the horizontal dipole antennas. Note that $\mathbf{C}_4$ is the conjugate transpose of $\mathbf{C}_3$.

The adaptive technique uses the property that the interfering signals received by the horizontal dipole antenna correlate with those received by the vertical antennas. The magnitudes of the cross-correlation coefficients in $\mathbf{C}_3$ and $\mathbf{C}_4$ would have an impact on the performance of the adaptive system. From $\mathbf{C}_3$, one can observe that $r_{1j} > r_{2j}$ and $r_{4j} > r_{3j}$ for j = 5, 6, 7, 8, 9, 10. The first inequality indicates that the output from the first horizontal dipole antenna was correlated with the outputs from the VPAs better than the output from the second horizontal dipole antenna. The second

Table II Magnitudes and Phases of 10 x 10 Covariance Matrix

a. Magnitudes (r_{ij})

1.000	0.476	0.616	0.837	0.670	0.639	0.587	0.579	0.534	0.539
0.476	1.000	0.752	0.441	0.399	0.385	0.415	0.333	0.372	0.237
0.616	0.752	1.000	0.716	0.344	0.299	0.364	0.312	0.376	0.265
0.837	0.441	0.716	1.000	0.567	0.550	0.523	0.562	0.527	0.577
0.670	0.399	0.344	0.567	1.000	0.924	0.907	0.867	0.822	0.785
0.639	0.385	0.299	0.550	0.924	1.000	0.927	0.905	0.859	0.826
0.587	0.415	0.364	0.523	0.907	0.927	1.000	0.895	0.890	0.846
0.579	0.333	0.312	0.562	0.867	0.905	0.895	1.000	0.917	0.900
0.534	0.372	0.376	0.527	0.822	0.859	0.890	0.917	1.000	0.909
0.539	0.237	0.265	0.577	0.785	0.826	0.846	0.900	0.909	1.000

b. Phases (θ_{ij})

0.0	-123.7	-38.1	-88.6	78.3	-58.7	-18.7	-76.4	172.3	37.8
123.7	0.0	90.8	58.5	115.4	-36.0	12.0	-47.7	-150.1	63.5
38.1	-90.8	0.0	-39.4	65.2	-79.7	-38.9	-90.1	162.1	36.4
88.6	-58.5	39.4	0.0	173.7	38.2	80.6	20.8	-84.9	138.3
-78.3	-115.4	-65.2	-173.7	0.0	-140.2	-94.7	-158.4	97.7	-46.1
58.7	36.0	79.7	-38.2	140.2	0.0	45.9	-15.8	-120.4	94.1
18.7	-12.0	38.9	-80.6	94.7	-45.9	0.0	-60.9	-164.8	48.5
76.4	47.7	90.1	-20.8	158.4	15.8	60.9	0.0	-103.7	112.2
-172.3	150.1	-162.1	84.9	-97.7	120.4	164.8	103.7	0.0	-144.1
-37.8	-63.5	-36.4	-138.3	46.1	-94.1	-48.5	-112.2	144.1	0.0

inequality indicates that the output from the fourth horizontal dipole antenna was correlated with the outputs from the VPAs better than the output from the third horizontal dipole antenna. The first and fourth antennas were horizontal dipoles perpendicular to the line of the vertical array, i.e., the coastline. The second and third antennas were horizontal dipoles parallel to the coastline. Hence, the observation indicates that during the experiment, the outputs from the dipoles perpendicular to the coastline were more highly correlated with the outputs from the VPAs than those parallel to the coastline. This report will show later that the system using the first or the fourth dipole would perform better than the one using the second or the third dipole.

Another observation in $\mathbf{C}_3$ and $\mathbf{C}_4$ is that the dipoles of the same orientation had similar cross-correlation coefficients with the vertical antennas. Antenna Elements 1 and 4, which were both perpendicular to the coastline, had cross-coefficients ranging from 0.527 to 0.670. Similarly, Antenna Elements 2 and 3, which were both parallel to the coastline, had cross-coefficients ranging from 0.237 to 0.415. Hence, we expect that the adaptive system using either one of the dipoles in the same orientation would have the same, or nearly the same, system performance.

The vertical array consisted of antenna elements that were identical. The horizontal array, however, consisted of antenna elements that were different in orientation. To gain a better understanding of the interfering signal environment, we carried out eigenanalyses of the submatrices $\mathbf{C}_1$ and $\mathbf{C}_2$, and the main matrix $\mathbf{C}$. Table III shows the eigenvalues of the two submatrices and the eigenvalues of the main matrix, respectively, in the order of decreasing relative magnitudes. In $\mathbf{C}_2$, the first eigenvalue is about 10.6 dB (1/0.088) larger than the second eigenvalue, whereas in $\mathbf{C}_1$, the first eigenvalue is only about 4.3 dB (1/0.371) larger than the second eigenvalue. The relative magnitudes of the first and second eigenvalues in $\mathbf{C}$ are similar to those in $\mathbf{C}_1$. As shown in Table III, the first eigenvalue in $\mathbf{C}$ about 4.1 dB (1/0.389) larger than the second eigenvalue. In a calibrated system, these eigenvalues could be used to determine the number of signal sources, including interference sources, present in the data.

Table III Relative Eigenvalues of Covariance Submatrices and Main Matrix

a. Relative Eigenvalues of 4x4 Submatrix $\mathbf{C}_1$:

1.000 0.371 0.118 0.061

b. Relative Eigenvalues of 6x6 Submatrix $\mathbf{C}_2$:

1.000 0.088 0.048 0.042 0.029 0.015

c. Relative Eigenvalues of 10x10 Matrix $\mathbf{C}$:

1.000 0.389 0.070 0.046 0.037 0.030 0.027 0.017 0.012 0.009

4. Adaptive System Configuration and Adaptive Algorithms

Figure 2 shows a block diagram of the adaptive system used for interference suppression. The main channels consist of the vertical monopole antennas and associated receiving systems, and the auxiliary channels consist of the horizontal dipole antennas and associated receiving systems. The inputs to the adaptive system can be divided into two parts; inputs from the main channels and inputs from the auxiliary channels. The main channel input consists of the vertically polarized radar signal and the interfering signals. The auxiliary channel inputs consist of only the horizontally polarized interfering signals. Normally, the outputs from the vertical antennas are combined in a specified manner (i.e, beamformed) to produce an output associated with a main beam at a specified look direction. In Figure 2, for example, we simply sum the outputs from the vertical antennas. Since the vertical antenna array is linear and uniform, this simple sum represents the output of the main beam in the boresight direction. The summed output is correlated in the adaptive system control unit in Figure 2 with the outputs from the auxiliary channels. From this correlation, we obtain a set of optimal weights for the outputs of the auxiliary channels. The weighted outputs are summed, and the summed output is then subtracted from the output of the main channel. In this

section, we derive an expression for the optimal weights, and we discuss methods that we used to estimate the weights.

The antenna array was not calibrated. To reduce the possibility of signal cancellation due to gain and phase mismatches at the outputs of the array elements, we equalized the gains and phases of the array elements with respect to those of the sixth element (Receive Element #19). For the equalization of the gains, we used the following steps: (1) from the outputs of the i-th antenna element, we estimated the auto-correlation r_{ii}, and (2) we multiplied the output of the i-th element with the square root of r_{66}/r_{ii}. For the equalization of the phases, we used a set of slightly different procedures: (1) from the outputs of the i-th and the 6-th antenna elements, we estimated the cross-correlation coefficient r_{i6}, and (2) we reduced the phase of the i-th element output by ξ_{i6}, where ξ_{i6} is the phase angle of r_{i6}. The gain and phase equalization above was carried out for all the antenna elements before the interference suppression. For simplicity, this equalization process is not shown in Figure 2.

For interference suppression, the output power of the system is minimized with respect to the real and imaginary parts of the weights for the horizontal antennas. From this minimization, we obtain a set of optimal weights. Before deriving the equation for the optimal weights, we make the following definitions:

$\mathbf{x}$ = a snapshot of the equalized array outputs at a specified range bin

$= (x_1, x_2, x_3, x_4, x_5, x_6, x_7, x_8, x_9, x_{10})^T$, where T denotes transpose

$\mathbf{a}$ = a snapshot of the equalized outputs form the auxiliary horizontal dipole antennas

$= (x_1, x_2, x_3, x_4)^T$

z = the sum of the equalized outputs of the vertically polarized antennas

$= x_5 + x_6 + x_7 + x_8 + x_9 + x_{10}$

$\mathbf{w}$ = a weight vector for the outputs of auxiliary antennas

$= (w_1, w_2, w_3, w_4)^T$

s = the output of the adaptive system

P = the signal power of the system output

As shown in Figure 2, the output of the adaptive system is given by

$$s = z - \mathbf{w}^H\mathbf{a} \tag{1}$$

and the signal power of the output is given by

$$P = |s|^2 = |z - \mathbf{w}^H\mathbf{a}|^2 \tag{2}$$

where $\mathbf{w}^H$ is the conjugate transpose of $\mathbf{w}$.

Differentiating P with respect to $\mathbf{w}$, equating the derivatives to zero, and taking the expected values on both sides of the equations, we then obtain the expression for the optimal weight vector as:

$$\mathbf{w} = \mathbf{R}_{aa}^{-1}\,\mathbf{r}_{az} \tag{3}$$

where $\mathbf{R}_{aa}^{-1}$ is the inverse of the covariance matrix of the outputs from the HPAs, and $\mathbf{r}_{az}$ is the cross-correlation between the outputs from the HPAs and the output of the main channel.

Two assumptions are made in the derivation of Equation (3), which is sometimes referred to as the unconstrained Wiener solution [6]. The first assumption is that the horizontal antennas do not receive the vertically polarized radar signals. The second assumption is that the interfering signals at the outputs of the horizontal antennas do not correlate with the transmitted radar signal at the output of the vertical antennas. Given these two assumptions, the sum of the weighted outputs from the horizontal antennas represents an optimal estimate of the interference component in the output of the main channel. A subtraction of this estimate from the main channel output would then result in a suppression of the interference from the output of the main channel.

The SMI method [4] was used to estimate the weights. This method requires the estimation of $\mathbf{R}_{aa}$ and $\mathbf{r}_{az}$ from samples in some selected range bins of the radar. For each range bin specified for interference suppression, two sets of range bins can be used. The first set is that of those at the very far ranges of the radar. The second set is that of those neighbouring to the range bin specified for interference suppression. For every waveform repetition interval, the weights are updated with Equation (3), using $\mathbf{R}_{aa}$ and $\mathbf{r}_{az}$ estimated from the samples in one of the two range bin sets. These samples are obtained from either the previous WRI or the current WRI. In this report, we used the previous WRI for the first set of range bins, and the current WRI for the second set of range bins. We refer to the method of using the first set of range bins as the fixed window method, and the method of using the second set of range bins as the sliding window method.

Fixed Window Method

The fixed window method uses the samples at the far ranges of the radar to estimate and update the weights. Let M be the range bin corresponding to the maximum range, or close to the maximum range, of the radar, and N be the number of range bins. For each WRI, we calculate the estimates of $\mathbf{R}_{aa}$ and $\mathbf{r}_{az}$ with

$$\hat{\boldsymbol{R}}_{aa} = \frac{1}{N} \sum_{k=M-N+1}^{M} \boldsymbol{a}_k \boldsymbol{a}_k^H \tag{4}$$

and

$$\hat{\boldsymbol{r}}_{az} = \frac{1}{N} \sum_{k=M-N+1}^{M} \boldsymbol{a}_k z_k^* \tag{5}$$

where $\mathbf{a}_k$ represents a snapshot of the horizontal array outputs at range bin k, and z_k represents the summed output of the vertical array also at range bin k, both from the previous WRI. For the current set of radar data, we arbitrarily chose M=240 and N=60. For each WRI, the estimates $\hat{\mathbf{R}}_{aa}$ and $\hat{\mathbf{r}}_{az}$

are used in Equation (3) to compute the weight vector **w**. Note that the computed weight vector is the same for all range bins.

Sliding Window Method

The sliding window method uses the samples in range bins close to the range bin selected for interference suppression. The equations for calculating $\hat{\mathbf{R}}_{aa}$ and $\hat{\mathbf{r}}_{az}$ are the same as those in Equations (4) and (5), except that the summations on the right hand sides are from $k = N_S+5$ to $k = N_S+N+5$, where N_S denotes the range bin selected for interference suppression. The radar signals are normally strong at close range bins. Hence, the range of k is chosen to be at the far side of the selected range bin, with five guard cells between the selected range bin and the first range bin used to estimate $\mathbf{R}_{aa}$ and $\mathbf{r}_{az}$. For the current set of radar data, we arbitrarily chose $N_S=27$ and $N=60$. The sliding window method assumes the absence of target signals in the range bins used to estimate $\mathbf{R}_{aa}$ and $\mathbf{r}_{az}$. For each WRI, the estimates $\hat{\mathbf{R}}_{aa}$ and $\hat{\mathbf{r}}_{az}$ are obtained from the samples in the current WRI, and the weight vector **w** is then computed in Equation (3). Note that the computed weights depend on N_S, the range bin selected for interference suppression.

5. Power Spectra of Radar Data

The Fast Fourier Transform (FFT) algorithm is used to calculate the power spectral density (PSD) of the echo data at a given range bin. A Blackman window [7] is also applied to the time series to reduce the leakage of the spectral power from one frequency bin to neighbouring frequency bins. The PSD of the radar data is the squared magnitude of the FFT output at various frequency bins, and is known as the power spectrum or the Doppler spectrum. For the current set of data, we used a 1024-point FFT in the calculation. The FMICW radar had a WRF of 9.01 Hz. Hence, the coherent integration time (CIT) of the radar was 1.89 minutes. To minimize the fluctuation of the FFT output, we summed the power of the FFT output at each frequency bin over all the spectra of

non-overlapping data blocks. There were 24 power spectra available. Hence, we summed the power of the FFT output over a duration of 45.5 minutes. Since the data blocks were contiguous, the duration was also the radar observation period, sometimes termed as the dwell time of the radar. For calibration purposes, a strong signal with a Doppler frequency of about 4.46 Hz was injected into the radar data before the FFT. This calibration tone was used as a reference for scaling the PSDs of the outputs from the radar system.

Figure 3 shows the integrated spectra of the main channel output for range bin 27, which corresponds to the range centred at 33.2 km. From Figure 3, one can observe that there was severe interference in the radar data. Normally, the PSD of the data includes two spectral lines, referred to as the Bragg lines, representing the first-order sea echoes. These two spectral lines are the result of resonant scattering of the radar signal by the approaching and receding ocean waves that have a wavelength equal to one half of the radar wavelength [8]. In the absence of ocean currents, the Bragg lines have Doppler frequencies [8] at

$$f_B = \pm \sqrt{\frac{g}{\pi\lambda}} \tag{6}$$

where g is the gravitational acceleration ($g = 9.81$ m/s^2), and λ is the radar wavelength (λ=c/f). Note that the '+' and '-' signs in Equation (6) indicate that the Bragg lines are scattered back, respectively, by the approaching and receding ocean waves. At the radar frequency of 5.811 MHz, the frequencies of the Bragg lines are ±0.246 Hz. These Bragg lines usually dominate the PSD of the output data from the main channel. However, because of the severe interference, the Bragg lines could not be observed in Figure 3. Note that the signal at about 4.46 Hz in Figure 3 is the calibration signal. This signal will also be shown in all subsequent PSD plots.

The integrated spectra of the four auxiliary channel outputs are shown in Figure 4, also for range bin 27. The four spectra exhibit similar shapes as the spectra from the main channel. Hence, there was also severe interference in the four auxiliary antenna channels.

The interference source was likely external. Data taken at night from a spectrum monitor at Cape Race, Newfoundland indicated the presence of a strong signal at 5.81 MHz. The observed interference in the radar experiment also appeared in all range bins.

6. Experimental Results

Before we present the results from the interference suppression, we need to define the measures of system performance. Two performance indicators were used in this report:

(i) The ratio of interference-plus-noise powers (RINP) before and after interference suppression;

(ii) The Bragg-to-interference-plus-noise ratios (BINRs) before and after interference suppression.

The interference-plus-noise power (INP) in the radar data was obtained by summing all the samples in the PSD, excluding those in the frequency bins of the Bragg lines and the frequency bin of the calibration tone. If P_b and P_a were the INP estimates before and after the interference suppression (with respect to the same calibration tone), then we calculated the first performance indicator as

$$\text{RINP} = P_b / P_a \tag{7}$$

The second performance indicator was originally defined as the change of BINRs before and after interference suppression. The Bragg lines, in many ways, behave like target signals. The change of BINRs would provide a good indication of the performance improvement of the radar for target detection. However, as shown in Figure 3, the Bragg lines were not observable in the Doppler spectrum of the data before interference suppression. Hence, we could only assume that the BINRs

for the approaching and the receding Bragg lines, denoted by ABINR and RBINR, respectively, were 0 dB or less in the data before interference suppression. We used, instead, the BINRs after interference suppression to indicate the improvement of the detection performance. Normally, the HFSWR spectrum also has a second-order sea clutter continuum around the Doppler bins of the Bragg lines, representing the second-order sea echoes of the radar [8]. To minimize the effect of the second-order sea clutter on BINRs, we define BINR, in decibel scale, as:

$$BINR = 10 \log_{10} S_B - \frac{1}{2} \left(10 \log_{10} S_{BL} + 10 \log_{10} S_{BR} \right) \tag{8}$$

where S_B is the power spectral density of a specified Bragg line, and S_{BL} and S_{BR} are the power spectral densities on the left and right sides of the Bragg line. To estimate S_{BL} and S_{BR}, we use the following expression:

$$S_{BL} = \frac{1}{P} \sum_{n=n_B-(3P-1)/2}^{n_B-(P+1)/2} S_n \tag{9}$$

and

$$S_{BR} = \frac{1}{P} \sum_{n=n_B+(P+1)/2}^{n_B+(3P-1)/2} S_n \tag{10}$$

where P is the width of the Doppler interval over which we sum the spectral power densities, n is the index of the Doppler bin number, S_n is the power spectral density at Doppler bin n, and n_B is the Doppler bin number where the selected Bragg line appears. For the current set of data, the Doppler width, P, was chosen to be 7. Since the Bragg lines could be shifted away from the expected Doppler frequencies due to the presence of ocean currents [8], we also needed to search for the maximum power spectral density around the expected Doppler bins before we could determine what n_B was for the Bragg line. This search for S_B was also incorporated in the estimation of BINR.

6.1 Fixed Window Method

In this section, we present the results of using the fixed window method in conjunction with the following combinations of auxiliary horizontal dipole antennas:

(1) One horizontal dipole, two different orientations;
(2) Two horizontal dipoles, three different combinations of orientation and location; and
(3) Four horizontal dipole antennas.

The data shown in Figures 3 and 4 were used to evaluate the effectiveness of the adaptive systems. Note that the range bin selected was 27, corresponding to the range centred at 33.2 km.

6.1.1 Adaptive System Using One Horizontal Dipole Antenna

We first examined the effectiveness of the system using one horizontal dipole antenna. Figure 5 shows the integrated spectra of the output from the system using Antenna Element 1. In comparing Figure 5 with Figure 3, one can observe that the interference was suppressed substantially. The first-order sea echoes, which cannot be observed in Figure 3, are now clearly observable in Figure 5. The RINP in Figure 5 is 6.63 dB. The BINRs, which are 0 dB or less in Figure 3, are now 9.03 dB and 11.31 dB, respectively, for the approaching and receding Bragg lines.

Figure 6 shows the integrated spectra of the output from the system using Antenna Element 2. In comparing Figure 6 with Figure 3, one can observe that the system has also suppressed the interference substantially. The Bragg lines are clearly visible in Figure 6. The RINP in this case is 4.44 dB. The BINRs are 3.28 dB and 9.84 dB, respectively, for the approaching and receding Bragg lines.

Compared to Figure 5, however, Figure 6 shows a lower Bragg line at 0.246 Hz and a slightly higher noise floor in the Doppler spectrum. This indicates that the adaptive system using Element

2 did not perform as well as the adaptive system using Element 1. This difference in system performance is consistent with the earlier observation in Section 3, where $r_{1j} > r_{2j}$ for j = 5 to 10.

We should point out that comparable results were obtained from the adaptive system using either Element 3 or Element 4. Again, consistent with the observation that $r_{4j} > r_{3j}$ for j = 5 to 10, the adaptive system using Element 3 did not perform as well as the system using Element 4.

6.1.2 Adaptive System Using Two Horizontal Dipole Antennas

We then studied the performance of the system using the following combinations of two horizontal dipole antennas:

(a) Orthogonal and collocated;
(b) Orthogonal and separated; and
(c) Parallel and separated

There were two adaptive systems with orthogonal and collocated dipole antennas. The first system used Elements 1 and 2, and the second system used Elements 3 and 4. Figures 7 and 8 show the summed PSD outputs from the two systems. Compared to the system using one horizontal element, these two-dipole systems provided a much more significant improvement in interference suppression. In these two figures, the interference is much more suppressed, and the Bragg lines are much more visible. The RINP is 10.29 dB in Figure 7 and 10.87 dB in Figure 8. The BINRs for the approaching and receding Bragg lines are 13.66 dB and 17.17 dB, respectively, in Figure 7. They are 14.71 dB and 18.92 dB, respectively, in Figure 8.

The system with two orthogonal but separated horizontal dipoles used element pairs 1 and 3 or 2 and 4. Figures 9 and 10 show the integrated spectra of the outputs from these systems. One can observe that the noise floor in Figure 9, calculated with Elements 1 and 3, is markedly higher

than that of Figure 10, calculated with Elements 2 and 4. The RINP is 8.71 dB in Figure 9, while it is 10.68 dB in Figure 10. The BINRs for the approaching and receding Bragg lines are 11.92 dB and 15.32 dB, respectively, in Figure 9, while they are 12.49 dB and 18.41 dB, respectively, in Figure 10. Compared to the systems with orthogonal and collocated horizontal dipoles, these systems with orthogonal and separated dipoles were not always as effective in interference suppression. While the PSD in Figure 10 is very much similar to those in Figures 7 and 8, the PSD in Figure 9 clearly exhibits a higher noise floor.

The system with two parallel and separated horizontal dipoles used element pair 1 and 4, or element pair 2 and 3. Figures 11 and 12, calculated with the first and the second pair, respectively, show the integrated spectra of the outputs from these two systems. The RINP is 8.02 dB in Figure 11 and 6.45 dB in Figure 12. The BINRs for the approaching and receding Bragg lines are, respectively, 8.52 dB and 13.50 dB in Figure 11, and 6.72 dB and 12.87 dB in Figure 12. The system using two parallel dipole antennas was hence less effective than those using two orthogonal dipole antennas.

The experimental results showed that the adaptive systems using two horizontal elements generally performed better than those using one horizontal antenna. Of the systems using two horizontal dipole antennas, the one that used two orthogonal and collocated dipoles consistently performed the best, and the one that used two parallel and separated dipoles performed the worst.

6.1.3 Adaptive System Using Four Horizontal Dipole Antennas

Finally, we evaluate the performance of the system using all four horizontal dipole antennas. Figure 13 shows the integrated spectra of the output from the system. This system by far offered the best performance. The RINP in this case is 13.01 dB. The BINRs are equal to 16.67 dB and 21.28 dB, respectively, for the approaching and receding Bragg lines.

6.1.4 Summary of System Performance

Tables IV and V summarise the performance of the systems studied in this section. The RINPs achieved by the different systems are shown in Table IV, and the BINRs are shown in Table V. The following observations can be made from the results shown in Table VI and V:

(i) The system performance generally improved with an increasing number of horizontal dipole antennas. Of the systems studied, the best performance was obtained from the one using all four horizontal dipole antennas. The RINP of this system was 13.01 dB. The BINRs were 16.67 dB and 21.28 dB, respectively, for the approaching and receding Bragg lines;

(ii) Of the systems with two horizontal elements, the system using two orthogonal and collocated dipoles was the best. The largest RINP of this system was 10.87 dB. The largest BINRs were 14.71 dB and 18.92 dB, respectively, for the approaching and receding Bragg lines;

(iii) The performance of the systems using one horizontal dipole antenna was significantly poorer than that of the systems using two or more horizontal dipole antennas. The largest RINP achieved by this system was 6.63 dB. The largest BINRs were 9.03 dB and 11.31 dB, respectively, for the approaching and receding Bragg lines.

Table IV Ratio of Interference-plus-Noise Powers (RINP) before and after Interference Suppression with Fixed Window Method

Adaptive System No.	No. of Horizontal Antennas	Antenna Element No.	Antenna Orientation and Location	RINP (dB)
1	1	1	Perpendicular to the coastline	6.63
2	1	2	Parallel to the coastline	4.44
3	2	1,2	Orthogonal & Collocated	10.29
4	2	3,4	Orthogonal & Collocated	10.87
5	2	1,3	Orthogonal & Separated	8.71
6	2	2,4	Orthogonal & Separated	10.68
7	2	1,4	Parallel & Separated	8.02
8	2	2,3	Parallel & Separated	6.45
9	4	1,2,3,4	Two Separate Crosses	13.01

Table V Approaching and Receding Bragg-to-Interference-plus-Noise Ratios (ABINR and RBINR) at Range 33.2 km before and after Interference Suppression with Fixed Window Method

Adaptive System No.	No. of Horizontal Elements	Antenna Element No.	Antenna Orientation and Location	ABINR (dB)	RBINR (dB)
*	0			<0	<0
1	1	1	Perpendicular to the coastline	9.03	11.31
2	1	2	Parallel to the coastline	3.28	9.84
3	2	1,2	Orthogonal & Collocated	13.66	17.17
4	2	3,4	Orthogonal & Collocated	14.71	18.92
5	2	1,3	Orthogonal & Separated	11.92	15.32
6	2	2,4	Orthogonal & Separated	12.49	18.41
7	2	1,4	Parallel & Separated	8.52	13.50
8	2	2,3	Parallel & Separated	6.72	12.87
9	4	1,2,3,4	Two Separate Crosses	16.67	21.28

* No interference suppression.

6.2 Sliding Window Method

Here, we present the results of using the sliding window method in conjunction with the combinations of the auxiliary horizontal dipole antennas discussed in Section 6.1. The data shown in Figures 3 and 4 were also used to evaluate the effectiveness of the adaptive systems. For brevity and for completeness, we simply show the integrated PSDs of the outputs from the various systems in Figures 14-22.

Tables VI and VII list the performance indicators of the adaptive systems extracted from the PSDs in Figures 14-22. In Table VI are the RINPs achieved by the various systems, and in Table VII are the corresponding BINRs for the approaching and receding Bragg lines. Similar to Section 6.1.4, one can derive the following observations from the results in Tables VI and VII:

(i) The system performance generally improved with an increasing number of horizontal dipole antennas. Of the systems studied, the best performance was obtained from the one using all the four horizontal dipoles. The RINP of this system was 17.40 dB. The BINRs were 19.85 dB and 24.66 dB, respectively, for the approaching and receding Bragg lines;

(ii) Of the systems with two horizontal elements, the system using two orthogonal and collocated dipole antennas consistently performed the best. The largest RINP of this system was 13.81 dB. The largest BINRs were 16.66 dB and 21.55 dB, respectively, for the approaching and receding Bragg lines;

(iii) The performance of the systems using one horizontal dipole antenna was significantly poorer than that of the systems using two or more horizontal dipole antennas. The largest RINP was 8.96 dB. The largest BINRs were 10.97 dB and 13.44 dB, respectively, for the approaching and receding Bragg lines.

Table VI Ratio of Interference-plus-Noise Powers (RINP) before and after Interference Suppression with Sliding Window Method

Adaptive System No.	No. of Horizontal Elements	Element No.	Antenna Orientation and Location	RINP (dB)
1	1	1	Perpendicular to the coastline	8.96
2	1	2	Parallel to the coastline	6.76
3	2	1,2	Orthogonal & Collocated	13.35
4	2	3,4	Orthogonal & Collocated	13.81
5	2	1,3	Orthogonal & Separated	12.11
6	2	2,4	Orthogonal & Separated	14.07
7	2	1,4	Parallel & Separated	10.87
8	2	2,3	Parallel & Separated	9.90
9	4	1,2,3,4	Two Separate Crosses	17.40

Table VII Approaching and Receding Bragg-to-Interference-plus-Noise Ratios (ABINR and RBINR) at Range 33.2 km before and after Interference Suppression with Sliding Window Method

Adaptive System No.	No. of Horizontal Elements	Element No.	Antenna Orientation and Location	ABINR (dB)	RBINR (dB)
*	0			<0	<0
1	1	1	Perpendicular to the coastline	10.97	13.44
2	1	2	Parallel to the coastline	4.74	11.15
3	2	1,2	Orthogonal & Collocated	16.08	19.49
4	2	3,4	Orthogonal & Collocated	16.66	21.55
5	2	1,3	Orthogonal & Separated	14.74	18.27
6	2	2,4	Orthogonal & Separated	14.37	21.95
7	2	1,4	Parallel & Separated	11.32	16.52
8	2	2,3	Parallel & Separated	9.14	15.76
9	4	1,2,3,4	Two Separate Crosses	19.85	24.66

* No interference suppression.

6.3 Performance Comparison of Two Adaptive Methods

In comparing Table IV with Table VI, one can observe that the sliding window method generally increased the RINP by about 2-4 dB over the fixed window method. Similarly, in comparing Table V with Table VII, one can observe that the sliding window method generally increased the BINRs by about 1-3 dB over the fixed window method. The best RINP and BINR improvements were achieved by Adaptive System No. 9, in which all the four horizontal dipole antennas were used in the interference suppression. The RINP in this case was increased by 4.39 dB, from 13.01 dB to 17.40 dB. The BINR for the approaching Bragg line, ABINR, was increased by 3.18 dB, from 16.67 to 18.85 dB, and the BINR for the receding Bragg line, RBINR, was increased by 3.38 dB, from 21.28 dB to 24.66 dB.

For each configuration of the auxiliary horizontal antennas, the sliding window method (Figures 14-22) can be compared with the fixed window method (Figures 5-13) to show the improvement of system performance. To facilitate this comparison, we plotted, side-by-side, the PSDs of the outputs from the same system using the two different methods. Figure 23 shows the results from Adaptive System No. 9 with all the four horizontal dipole antennas. In Figure 23(a) is the integrated spectra of the output from the system using the fixed window method, and in Figure 23(b) is the integrated spectra of the output from the same system using the sliding window method. From Figure 23, one can observe that the sliding window method lowered the noise floor by approximately 4 dB more than the fixed window method. The second-order sea echo, which cannot be observed in Figure 23(a), is now observable between the Bragg lines in Figure 23(b).

By lowering the noise floor, the sliding window method improves the signal-to-noise ratio in target detection. However, we should point out that there are also pitfalls in using the sliding window method. This method carries a larger computational load, and is more prone to artefacts in the outputs of the adaptive systems due to the presence of stronger radar signals in the selected range bins. The increase in the computational load is obvious from the structures of the adaptive algorithms. For each WRI, the fixed window method computes the weights only once for all range

bins, but the sliding window method has to compute the weights for each and every range bin. For the current set of data, we have not observed any artefacts in the outputs of the systems using the sliding window method, likely because no target signals were present in the range bins selected for the estimation of the weights. In practice, one does not know where a target is and may use its range bin to calculate the adaptive weights. Target signals in range bins next to the one selected for interference suppression are usually stronger than those at the far ranges. Hence, the sliding window method is more susceptible to artefacts at the output of the adaptive system than the fixed window method.

7. Conclusions and Recommendation

This report has presented the results of an experiment to study the effectiveness of an adaptive technique using auxiliary horizontal dipole antennas to suppress the skywave interference in HFSWR. The results showed that the technique was effective in suppressing the nighttime skywave interference. Two different adaptive methods, called the fixed and sliding window methods, were used to estimate and update the weights of the outputs of the auxiliary horizontal antennas. With the fixed window method, the interference-plus-noise power was reduced by up to 13 dB, and the Bragg-to-interference-plus-noise-ratio was increased by up to 21 dB. With the sliding window method, the INP was reduced by up to 17 dB, and the BINR was increased by up to 25 dB. In both methods, we also compared the effectiveness of the adaptive technique using one, two or four horizontal dipole antennas. We found that:

(i) The technique was most effective when all four horizontal dipoles were used;

(ii) Among the systems with two horizontal elements, the system using two orthogonal and collocated dipoles consistently performed the best; and

(iii) While the system using one horizontal dipole antenna worked against the observed

interference, the system performance was significantly poorer than the system using two or more horizontal dipole antennas.

The above results show that the adaptive technique can provide an effective means to alleviate the problem of skywave interference in a HFSWR.

Acknowledgements

The author would like to thank Mr. Barry Dawe of Northern Radar System Limited for supplying the radar data, and Dr. E. Hung of DREO for his assistance in this study.

References

1. Kenneth Davies, "Ionospheric Radio", Peter Peregrinus Ltd., London, U.K., 1990, p. 235.
2. S. Leinwoll, "Shortwave Propagation", John Lyder Publisher Inc., New York, 1959, p. 65.
3. J. M. Madden, "The Adaptive Suppression of Interference in HF Ground Wave Radar", **RADAR '87**, IEE International Conference, London, U.K., Oct. 19-21, 1987, pp. 98-102.
4. R.T. Compton, "Adaptive Antennas -- Concepts and Performance", Prentice Hall, Englewood Cliffs, New Jersey, 1988, p. 326.
5. Northern Radar Systems Limited -- Transmitter and Receiver Hardware Manuals, compiled by Desmond Power, January, 1995.
6. Widrow B, Glover J, McCool J, Kaunitz J, Williams C, Hearn R, Zeidler J, Dong E and Goodlin R, "Adaptive Noise Cancelling: Principles and Applications", Proceedings of IEEE, Vol. 63, No. 12, December 1975, p. 1692.
7. F.J. Harris, "On the Use of Windows for Harmonic Analysis with the Discrete Fourier Transform", Proceedings of the IEEE, Vol. 66, No. 1, January 1966, pp. 51-83.
8. D. E. Barrick, "Remote Sensing of Sea State by Radar", Chapter 12, in "Remote Sensing of Troposphere", Edited by V. E. Derr, GPO, Washington, DC, 1972.

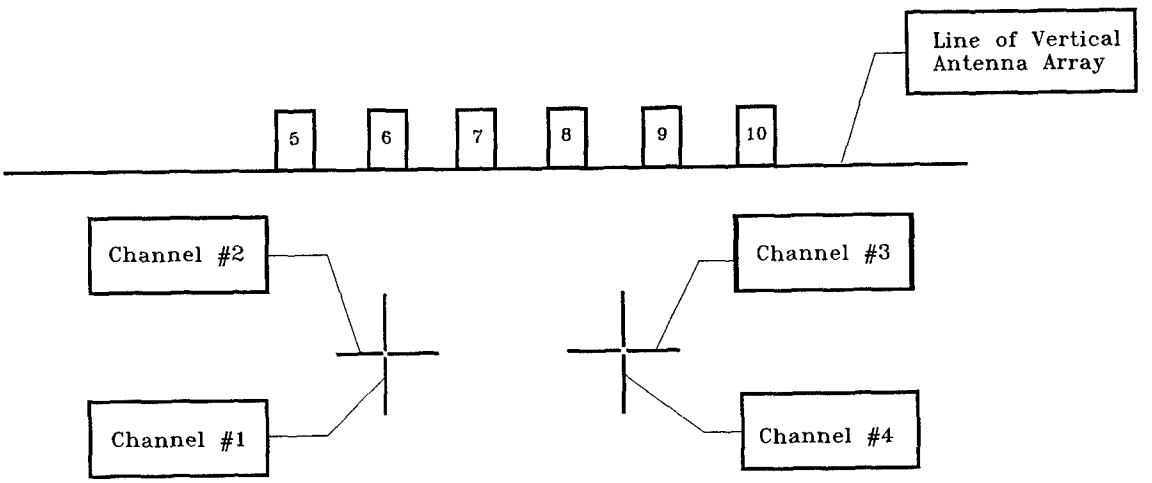

Figure 1 Receiving Antenna Configuration (Top View)

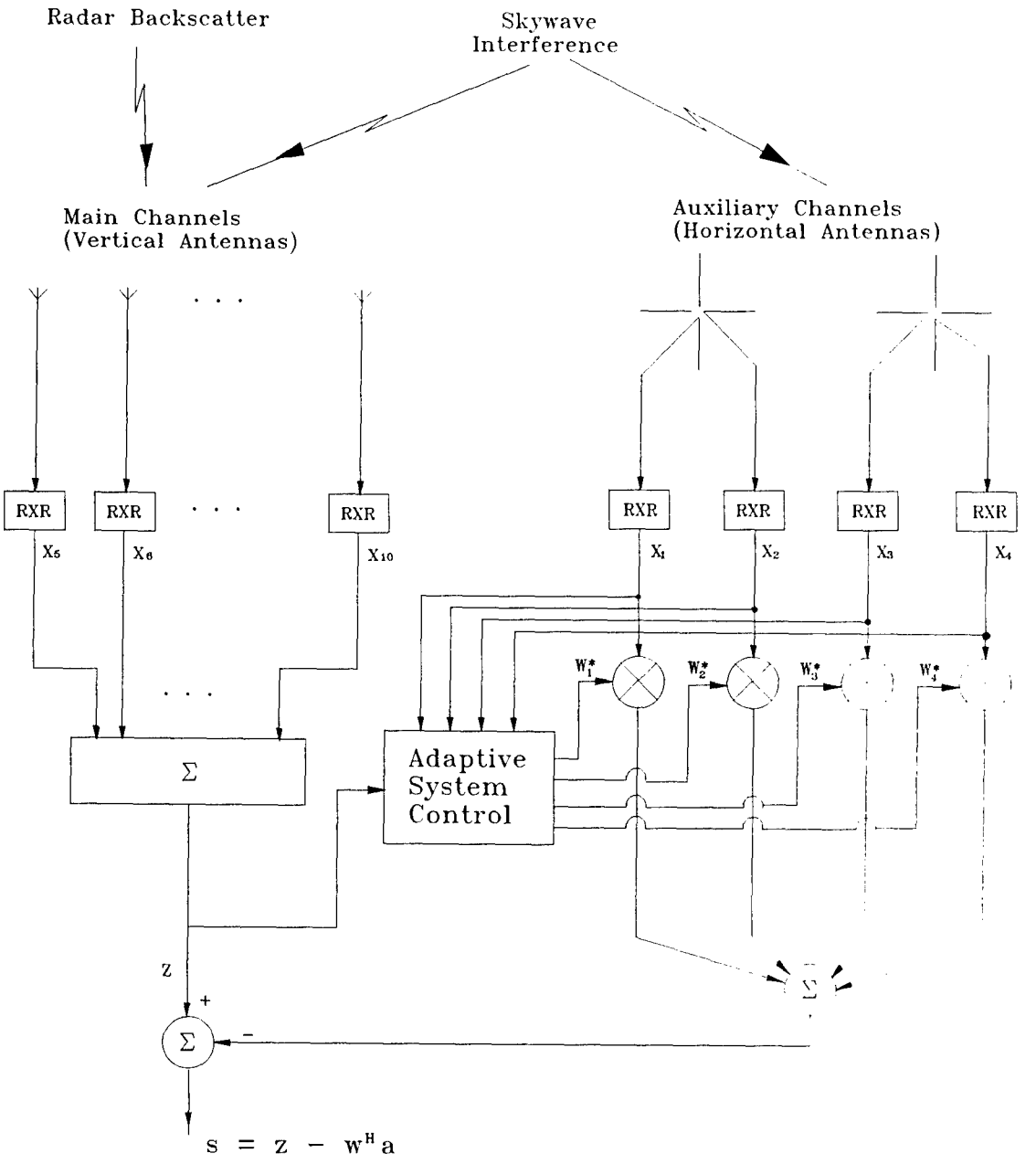

Figure 2 Adaptive System Configuration

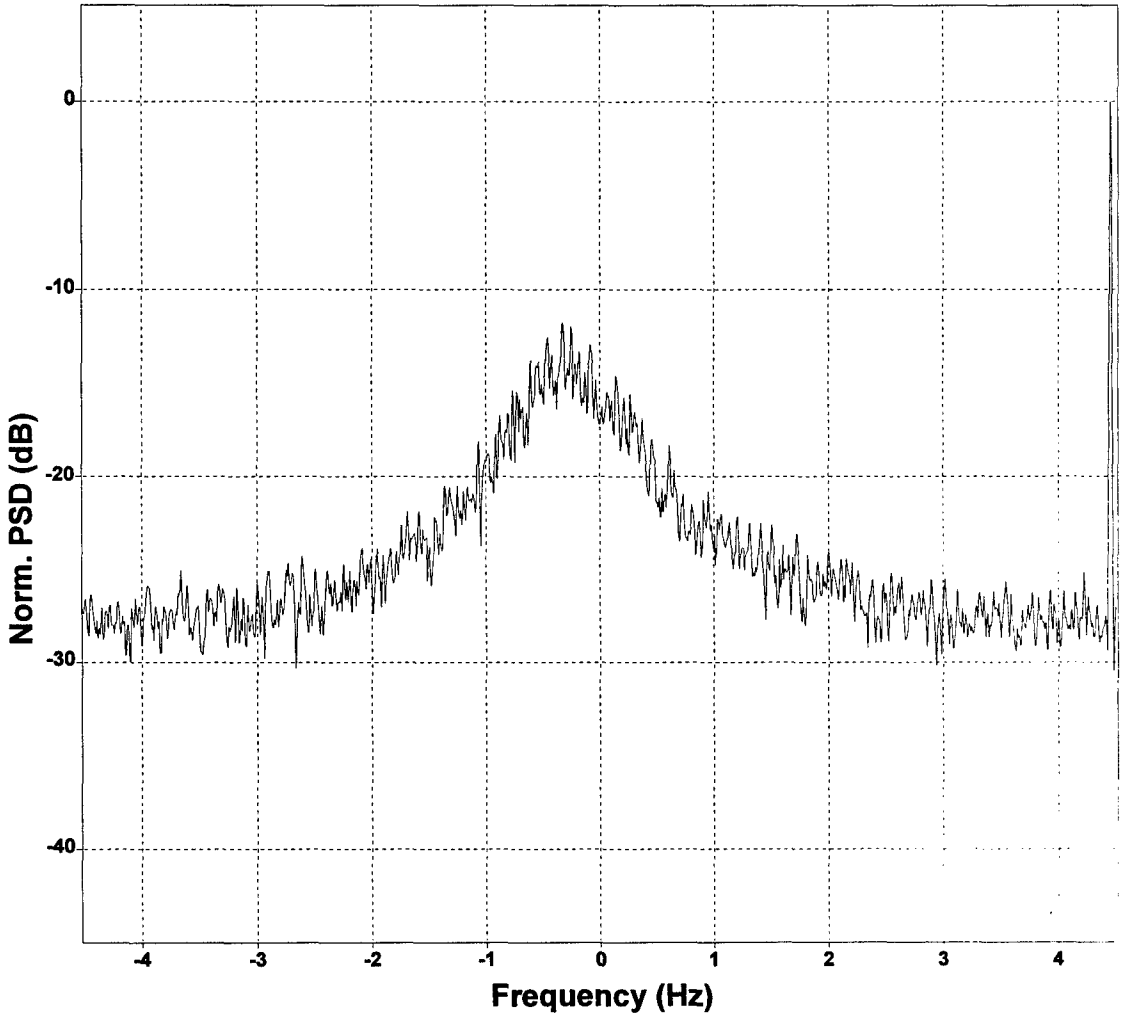

Figure 3 Normalized Power Spectral Density of Output Summed from Six Vertical Antennas (Range=33.2 km; 1024-point FFT with Blackman Window, CIT=114 seconds; Dwell Time=45.5 minutes)

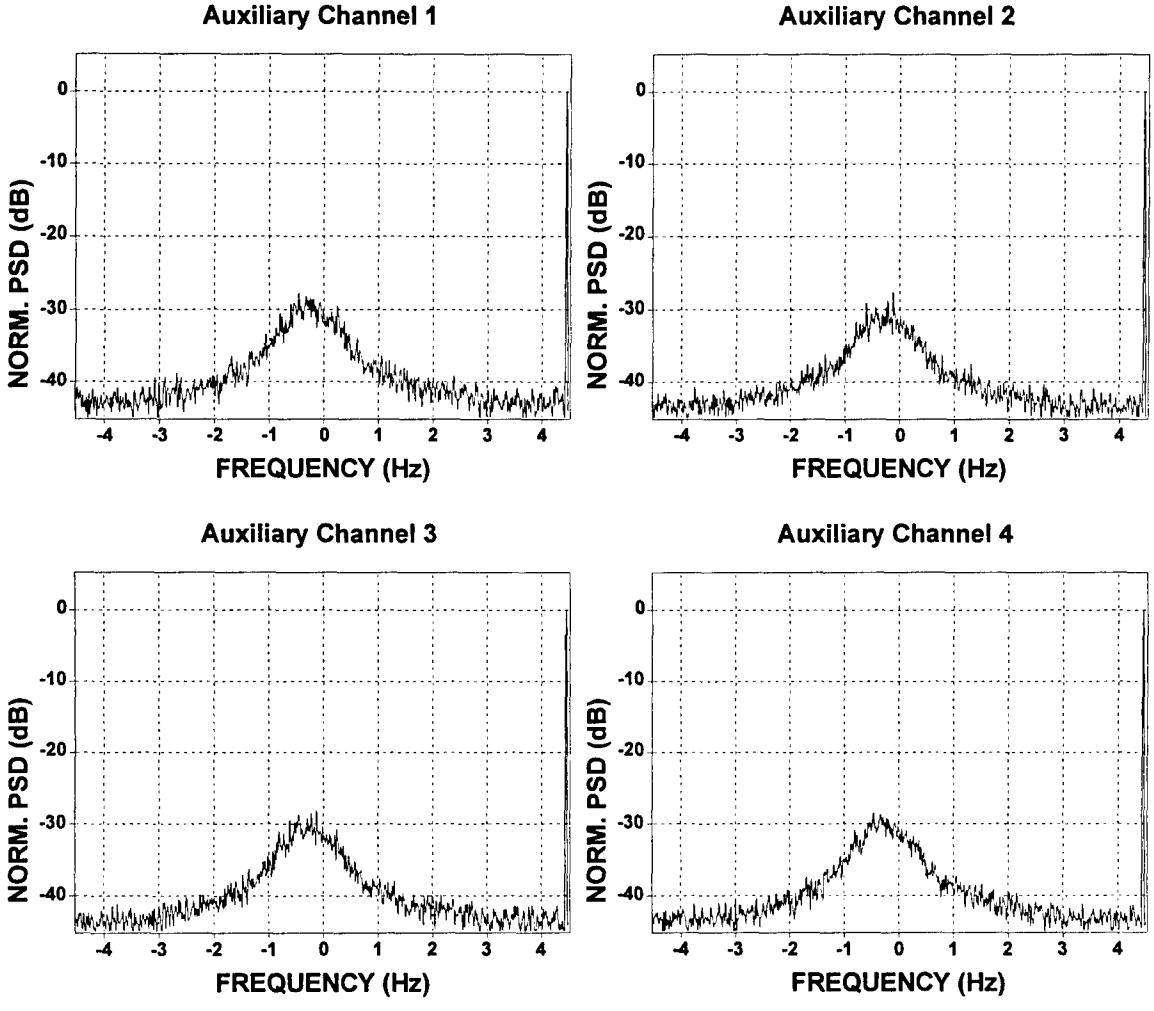

Figure 4 Normalized Power Spectral Densities of Outputs from Four Auxiliary Horizontal Dipole Antennas (Range=33.2 km; 1024-point FFT with Blackman Window, CIT=114 seconds; Dwell Time=45.5 minutes)

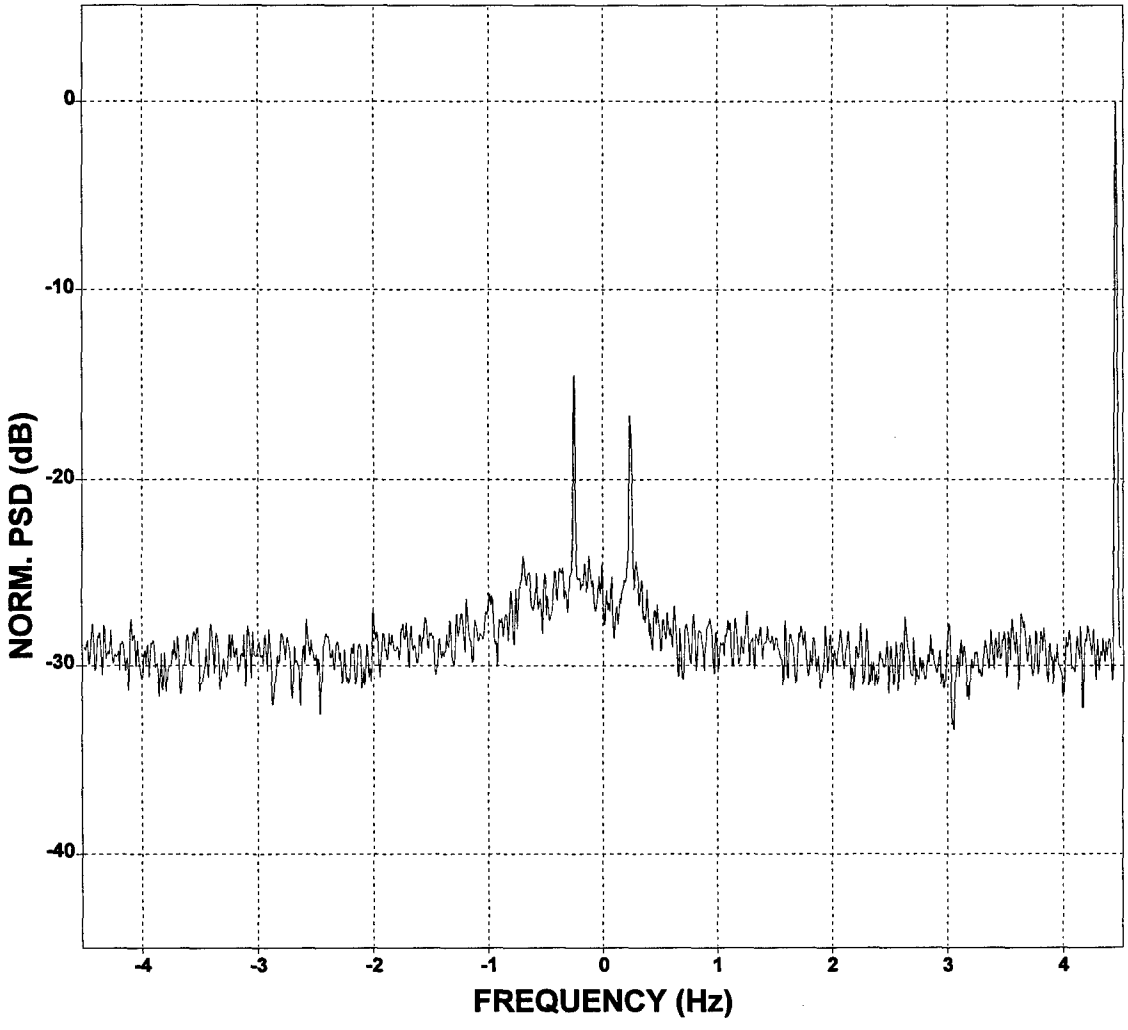

Figure 5 Normalized Power Spectral Density of Output from Adaptive System Using One Auxiliary Horizontal Dipole (Antenna Element 1, perpendicular to the coastline); Fixed Window Method was used to Estimate and Update Weight Coefficients

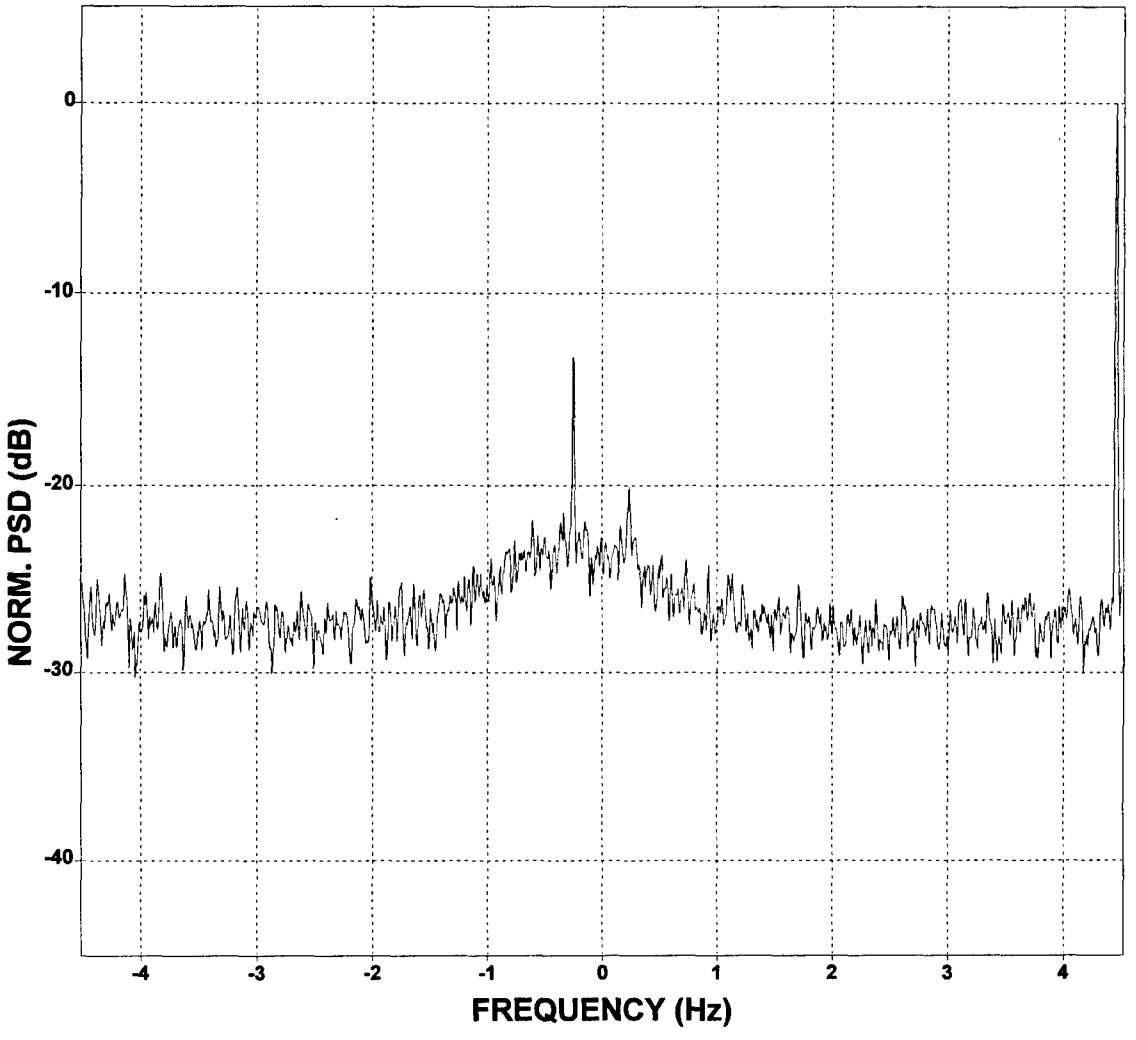

Figure 6 Normalized Power Spectral Density of Output from Adaptive System Using One Auxiliary Horizontal Dipole (Antenna Element 2, parallel to the coastline); Fixed Window Method was used to Estimate and Update Weight Coefficients

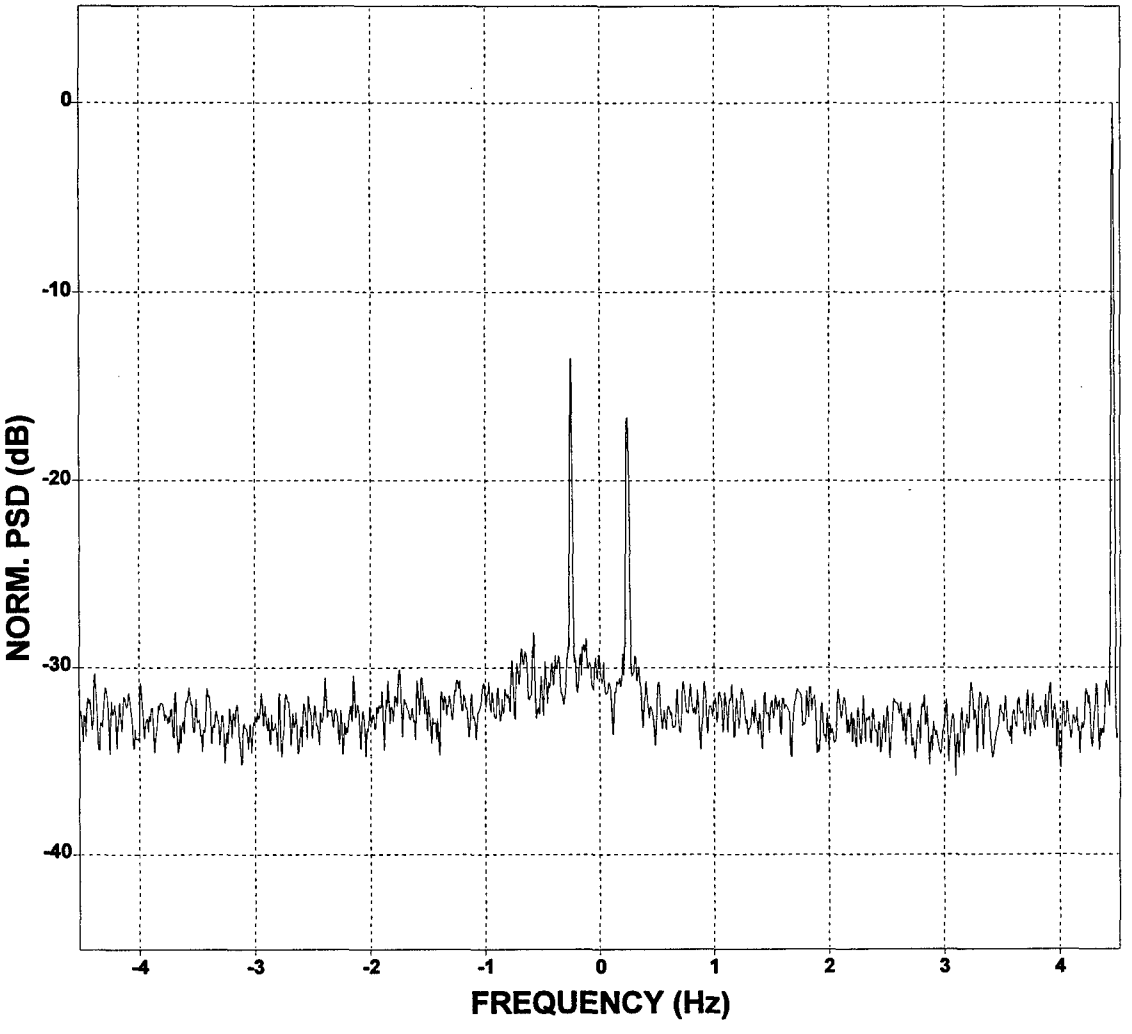

Figure 7 Normalized Power Spectral Density of Output from Adaptive System Using Two Auxiliary Horizontal Dipoles (Antenna Elements 1 and 2; orthogonal & collocated); Fixed Window Method was used to Estimate and Update Weight Coefficients

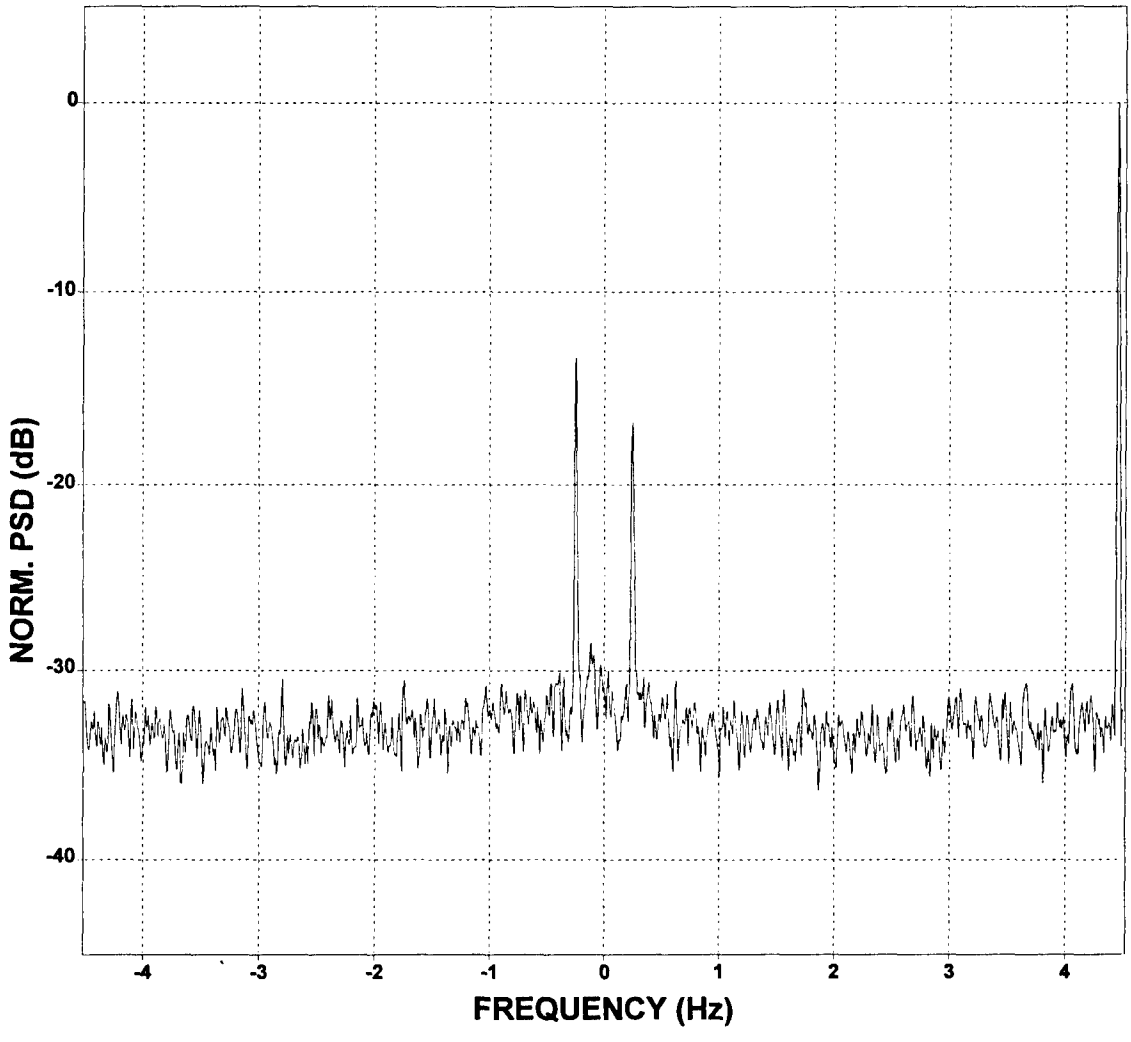

Figure 8 Normalized Power Spectral Density of Output from Adaptive System Using Two Auxiliary Horizontal Dipoles (Antenna Elements 3 and 4, orthogonal & collocated); Fixed Window Method was used to Estimate and Update Weight Coefficients

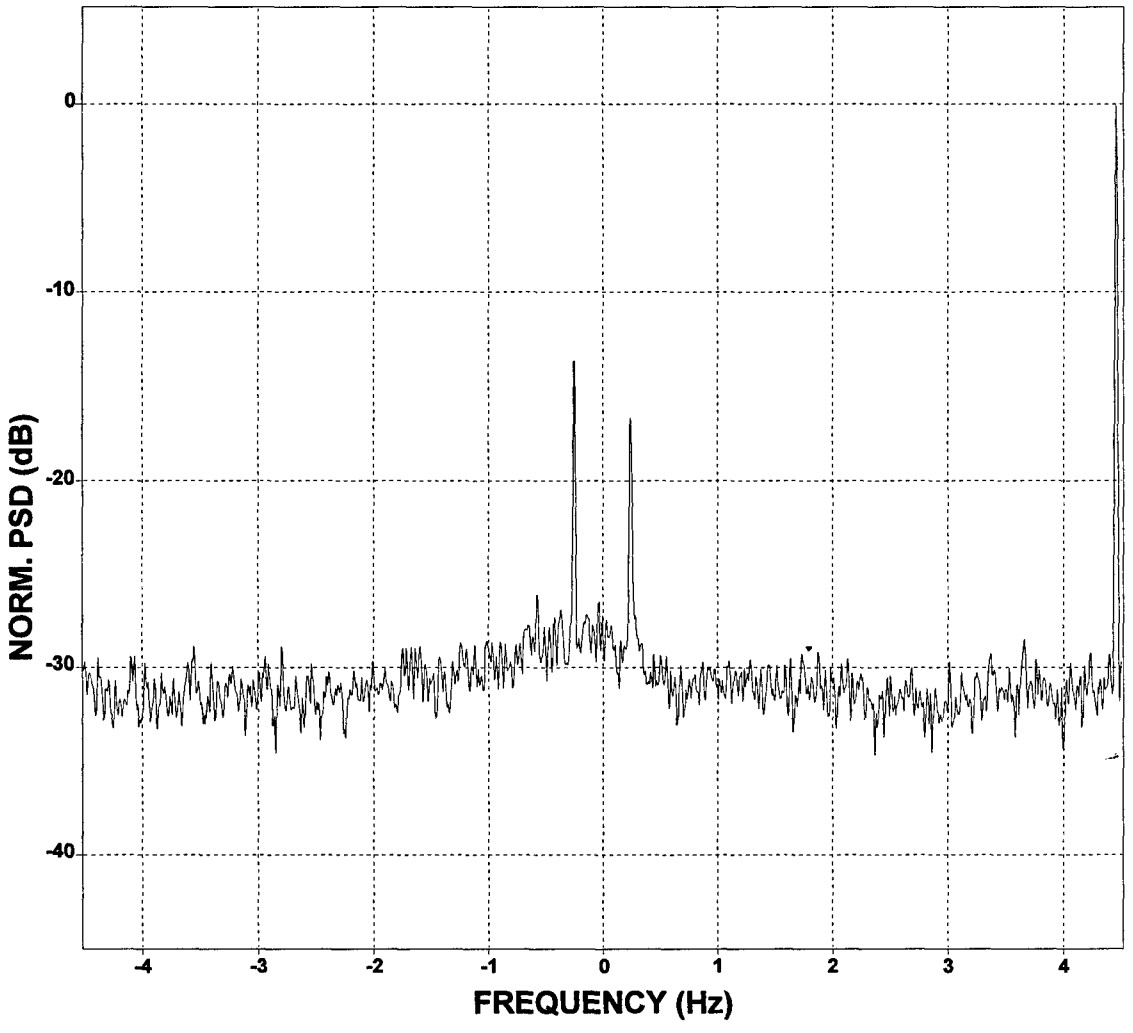

Figure 9 Normalized Power Spectral Density of Output from Adaptive System Using Two Auxiliary Horizontal Dipoles (Antenna Elements 1 and 3, orthogonal & separated); Fixed Window Method was used to Estimate and Update Weight Coefficients

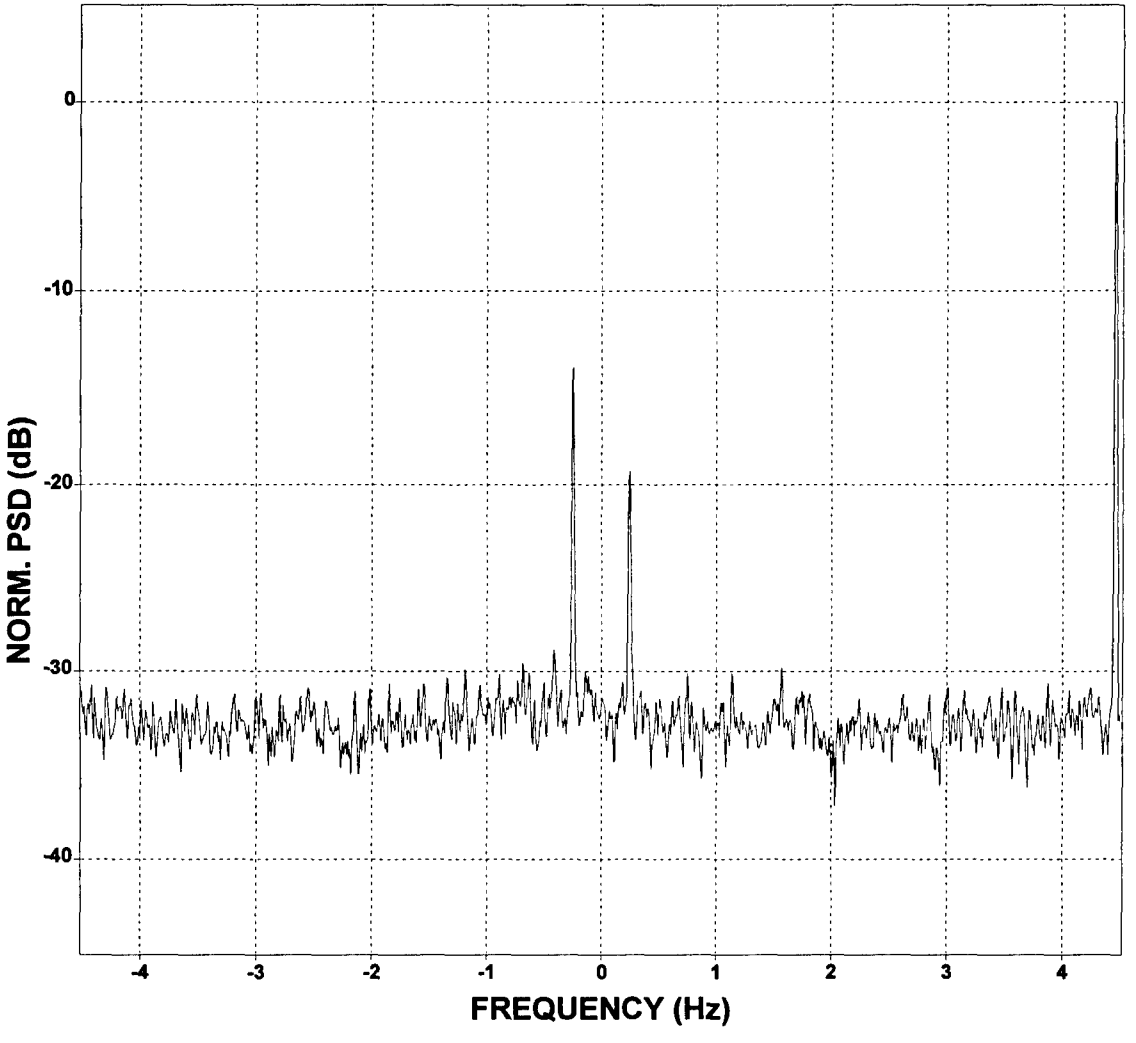

Figure 10 Normalized Power Spectral Density of Output from Adaptive System Using Two Auxiliary Horizontal Dipoles (Antenna Elements 2 and 4, orthogonal & separated); Fixed Window Method was used to Estimate and Update Weight Coefficients

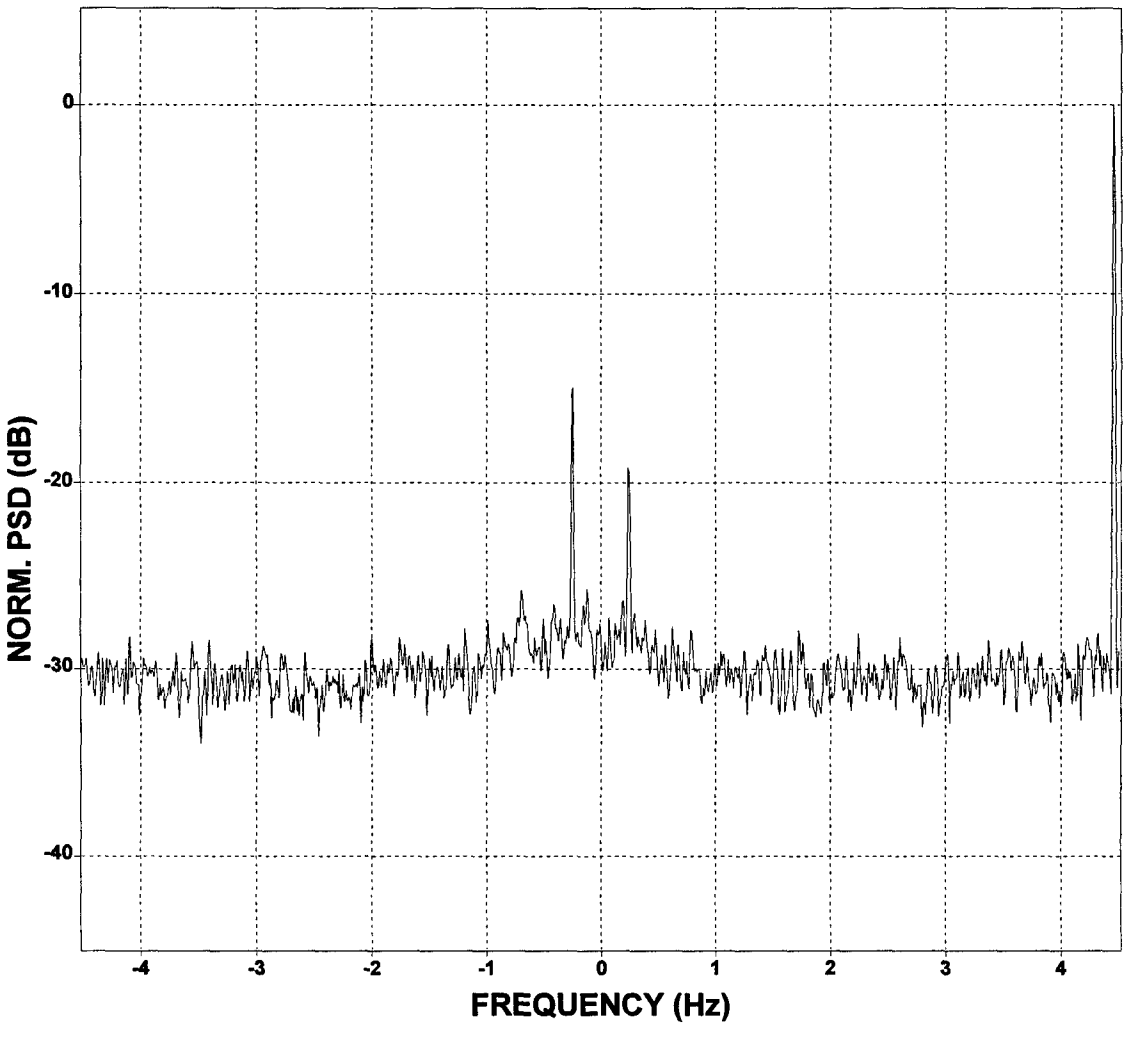

Figure 11 Normalized Power Spectral Density of Output from Adaptive System Using Two Auxiliary Horizontal Dipoles (Antenna Elements 1 and 4, parallel & separated); Fixed Window Method was used to Estimate and Update Weight Coefficients

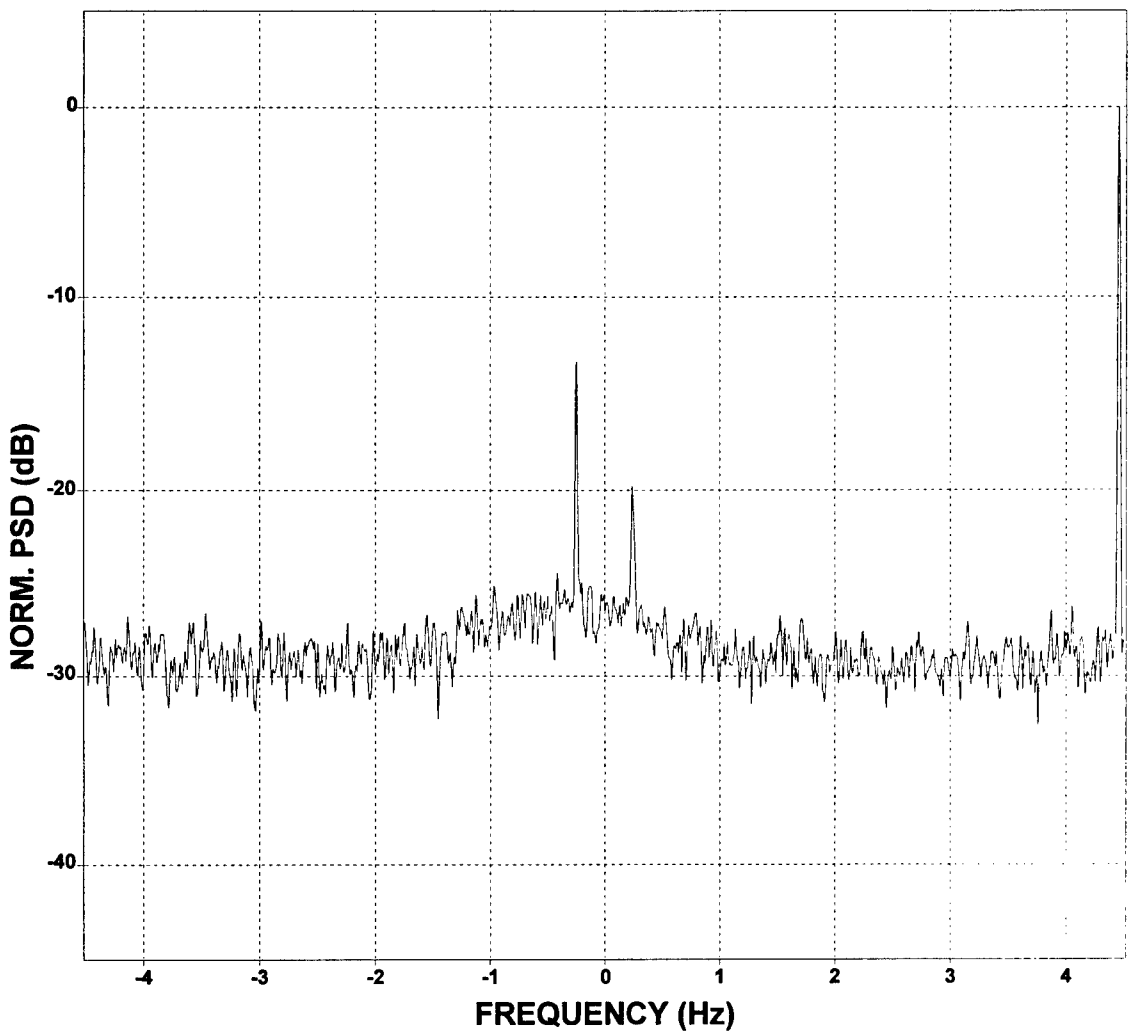

Figure 12 Normalized Power Spectral Density of Output from Adaptive System Using Two Auxiliary Horizontal Dipoles (Antenna Elements 2 and 3, parallel & separated); Fixed Window Method was used to Estimate and Update Weight Coefficients

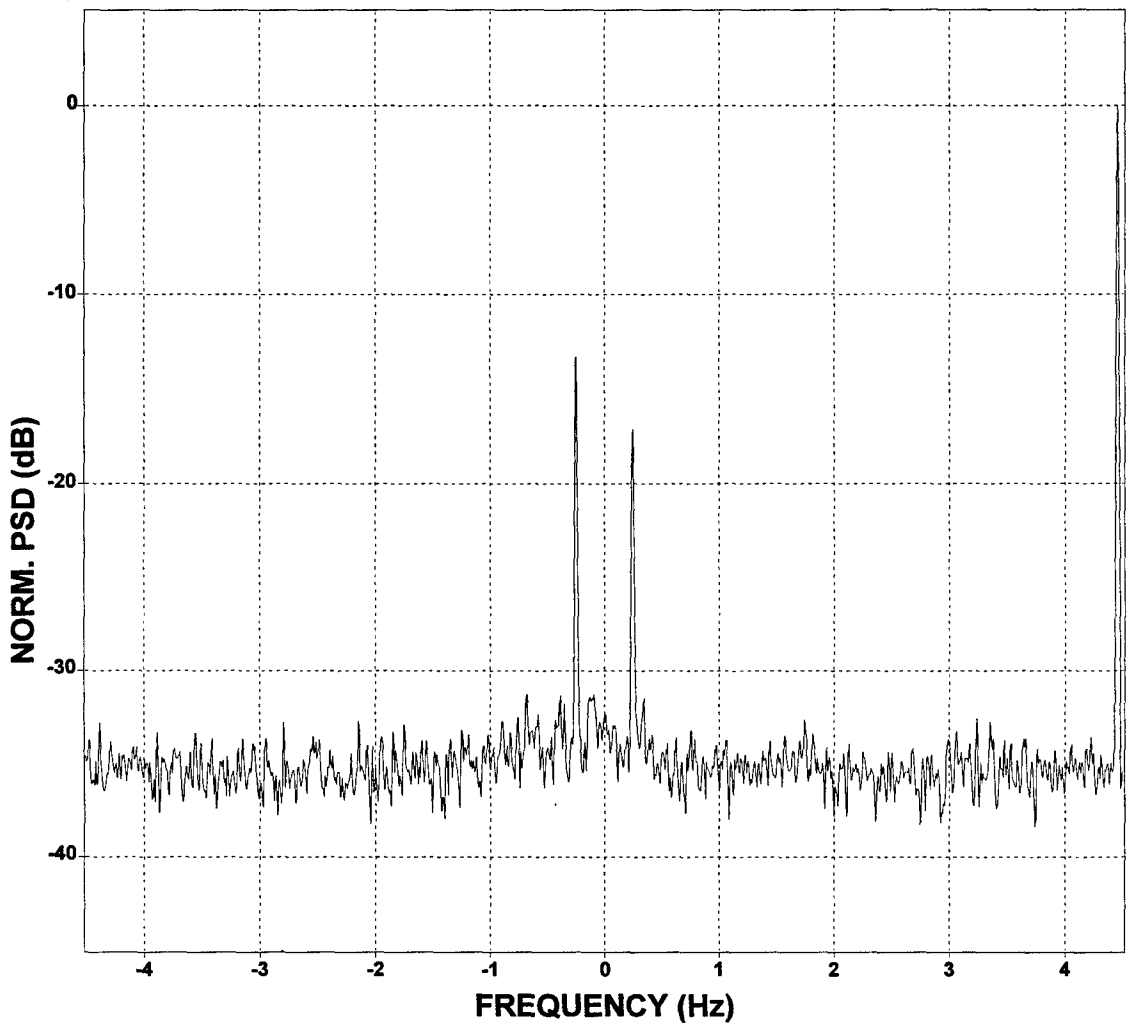

Figure 13 Normalized Power Spectral Density of Output from Adaptive System Using Four Auxiliary Horizontal Dipoles; Fixed Window Method was used to Estimate and Update Weight Coefficients

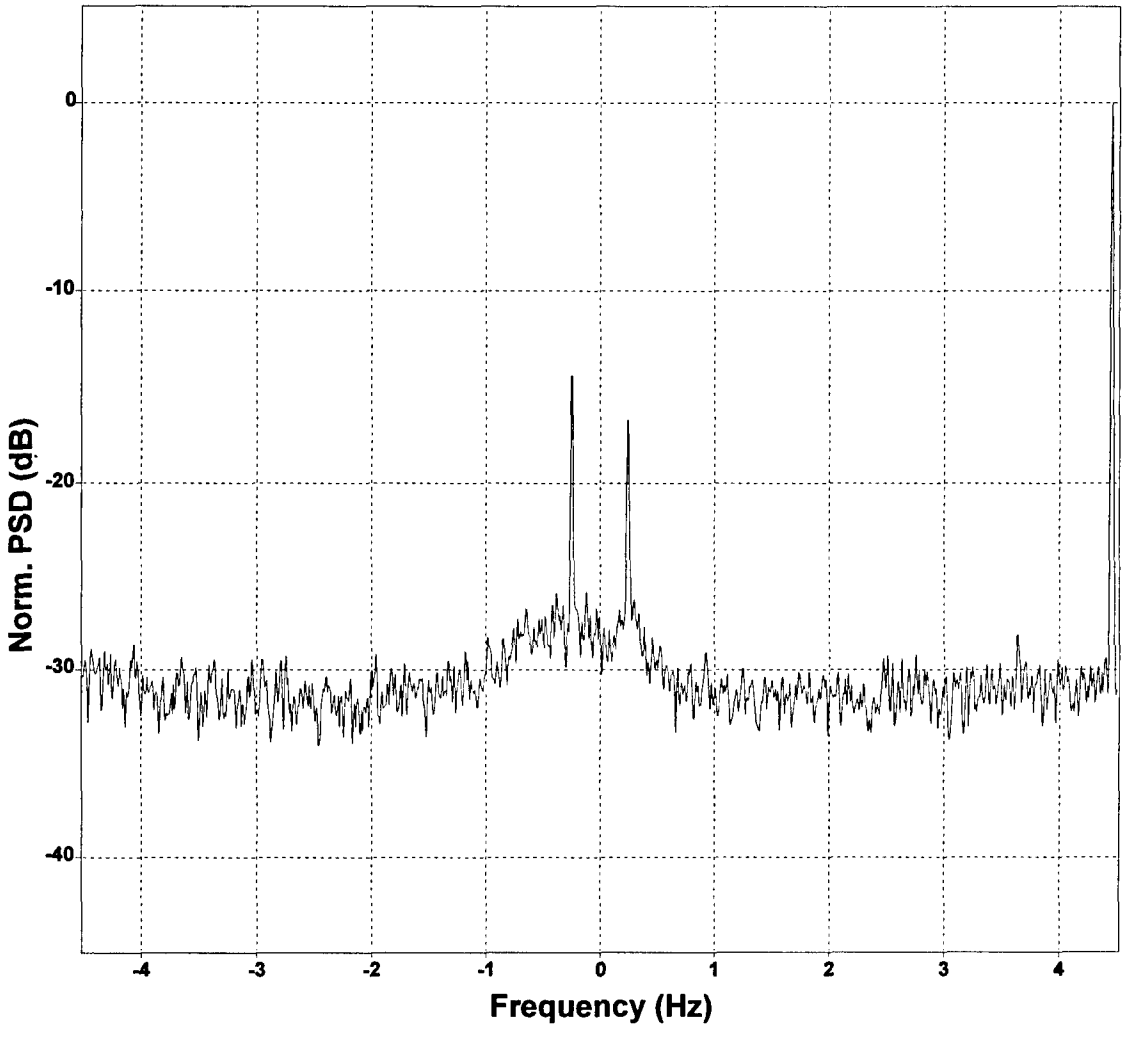

Figure 14 Normalized Power Spectral Density of Output from Adaptive System Using One Auxiliary Horizontal Dipole (Antenna Element 1, perpendicular to the coastline); Sliding Window Method was used to Estimate and Update Weight Coefficients

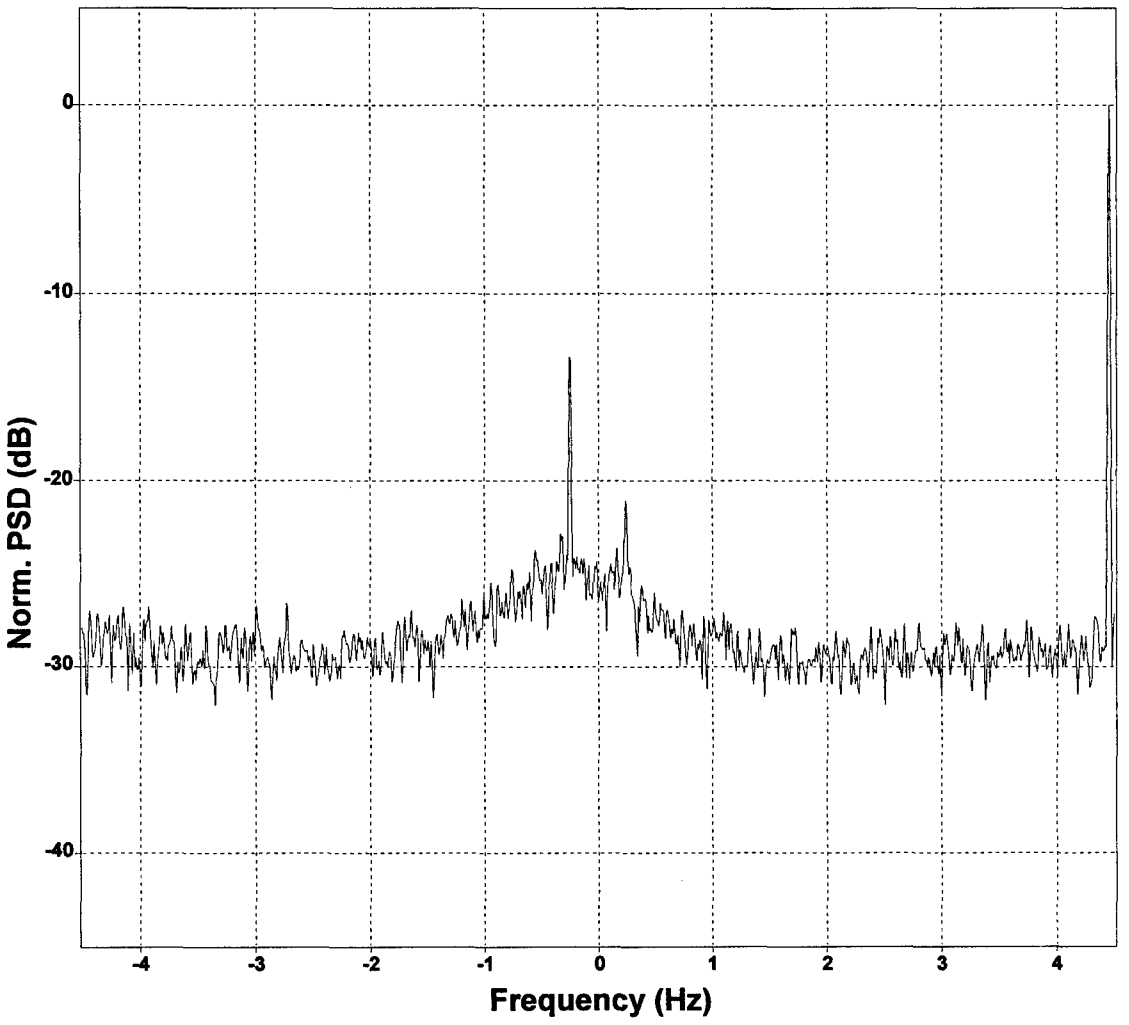

Figure 15 Normalized Power Spectral Density of Output from Adaptive System Using One Auxiliary Horizontal Dipole (Antenna Element 2, parallel to the coastline); Sliding Window Method was used to Estimate and Update Weight Coefficients

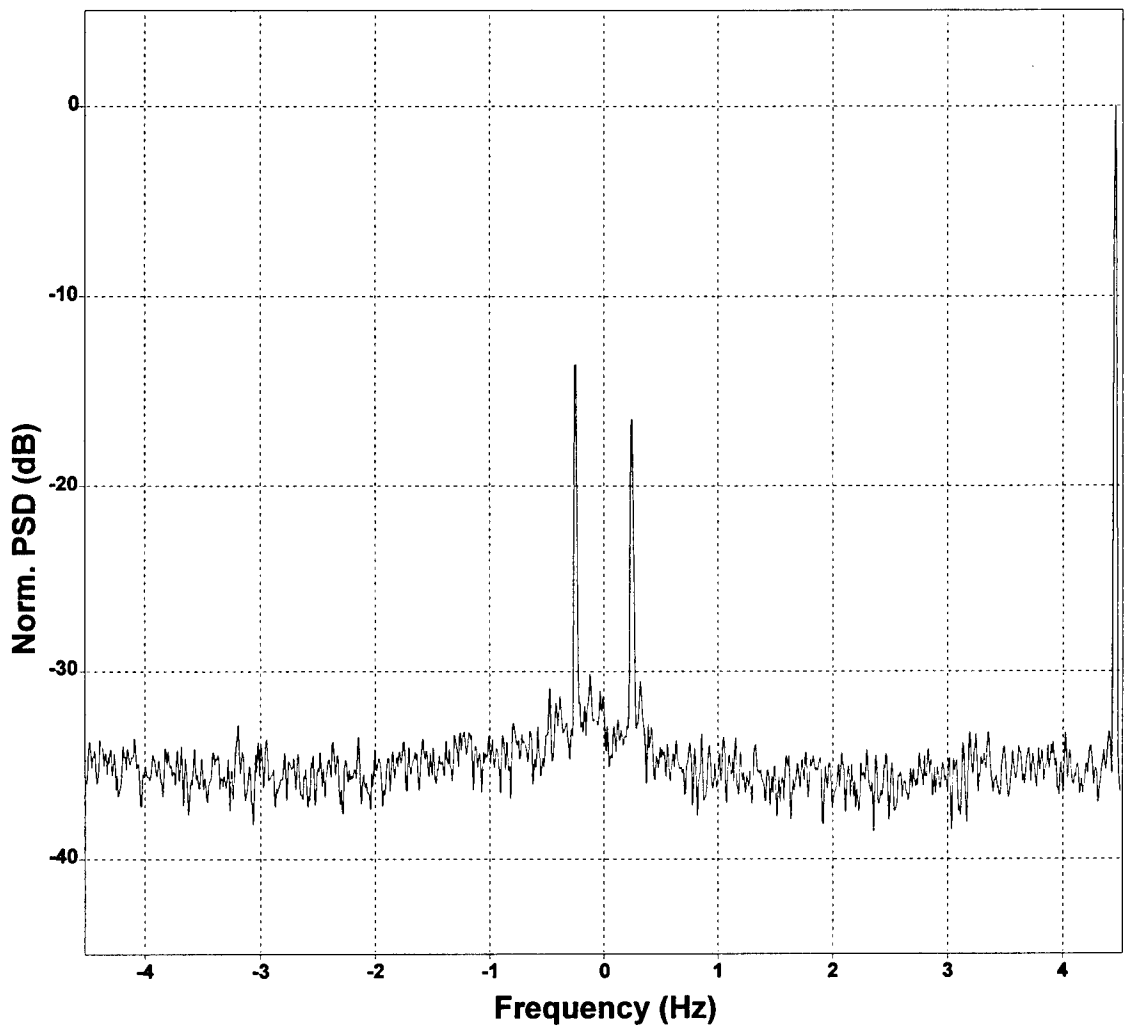

Figure 16 Normalized Power Spectral Density of Output from Adaptive System Using Two Auxiliary Horizontal Dipoles (Antenna Elements 1 and 2, orthogonal & collocated); Sliding Window Method was used to Estimate and Update Weight Coefficients

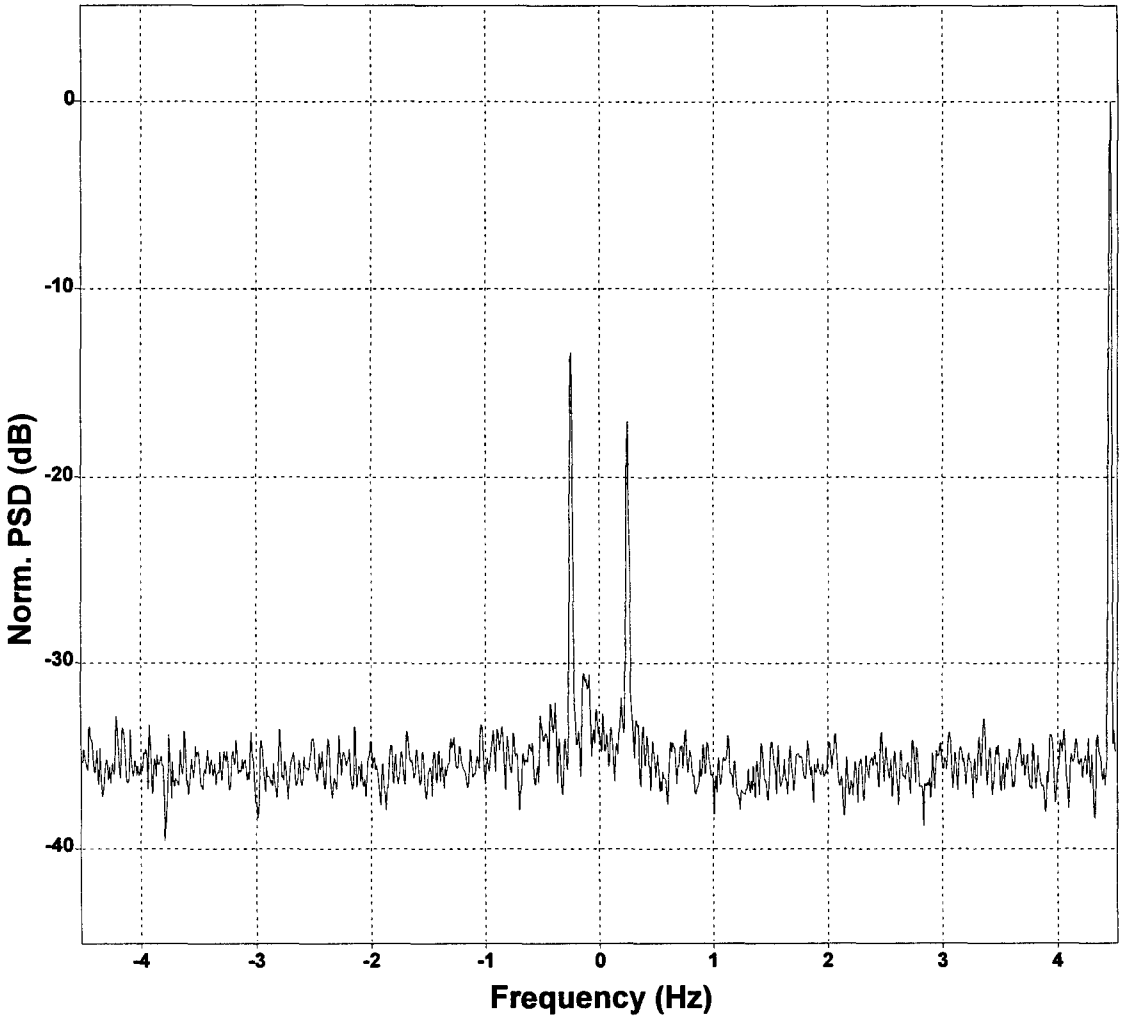

Figure 17 Normalized Power Spectral Density of Output from Adaptive System Using Two Auxiliary Horizontal Dipoles (Antenna Elements 3 and 4, orthogonal & collocated); Sliding Window Method was used to Estimate and Update Weight Coefficients

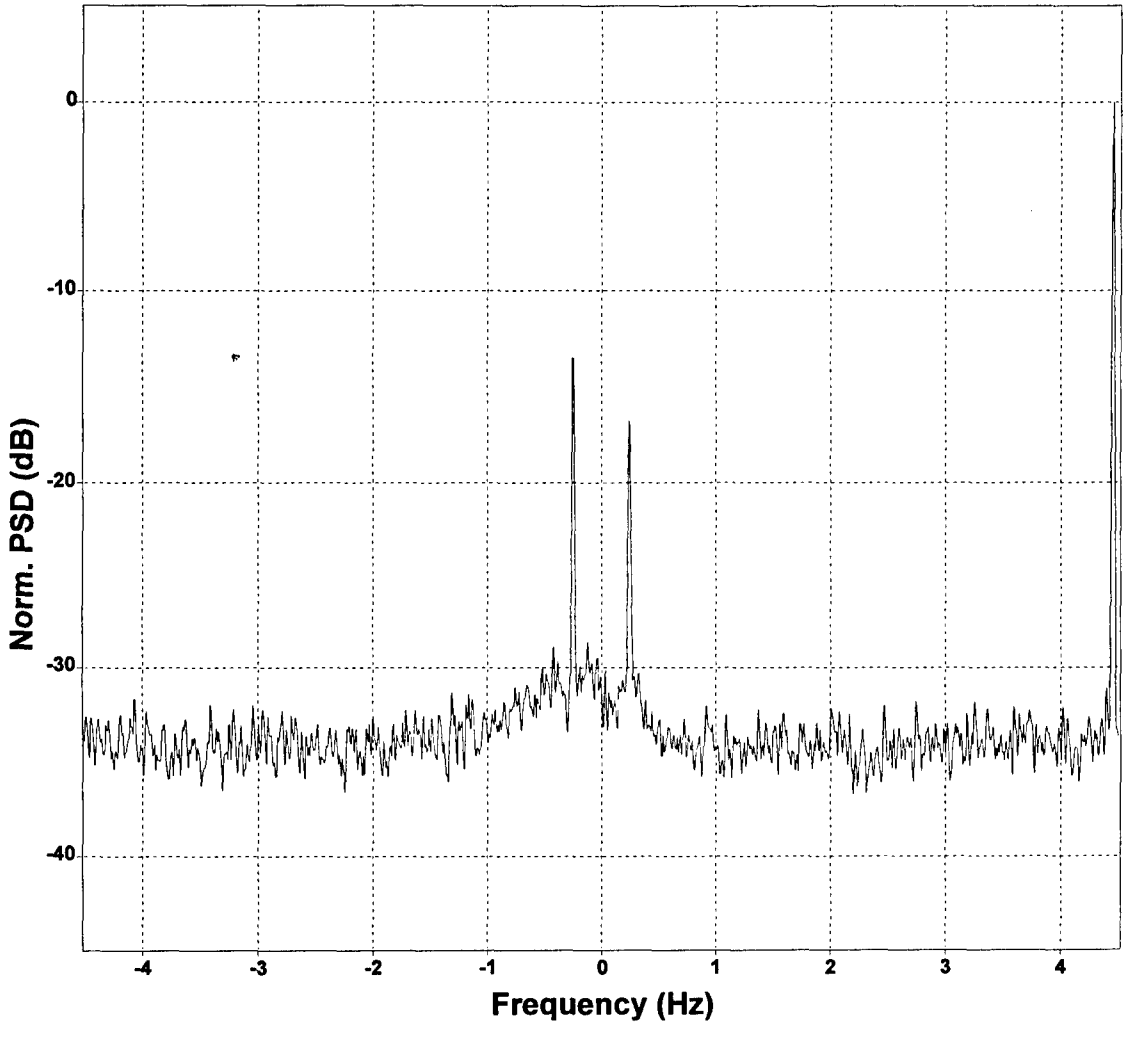

Figure 18 Normalized Power Spectral Density of Output from Adaptive System Using Two Auxiliary Horizontal Dipoles (Antenna Elements 1 and 3, orthogonal & separated); Sliding Window Method was used to Estimate and Update Weight Coefficients

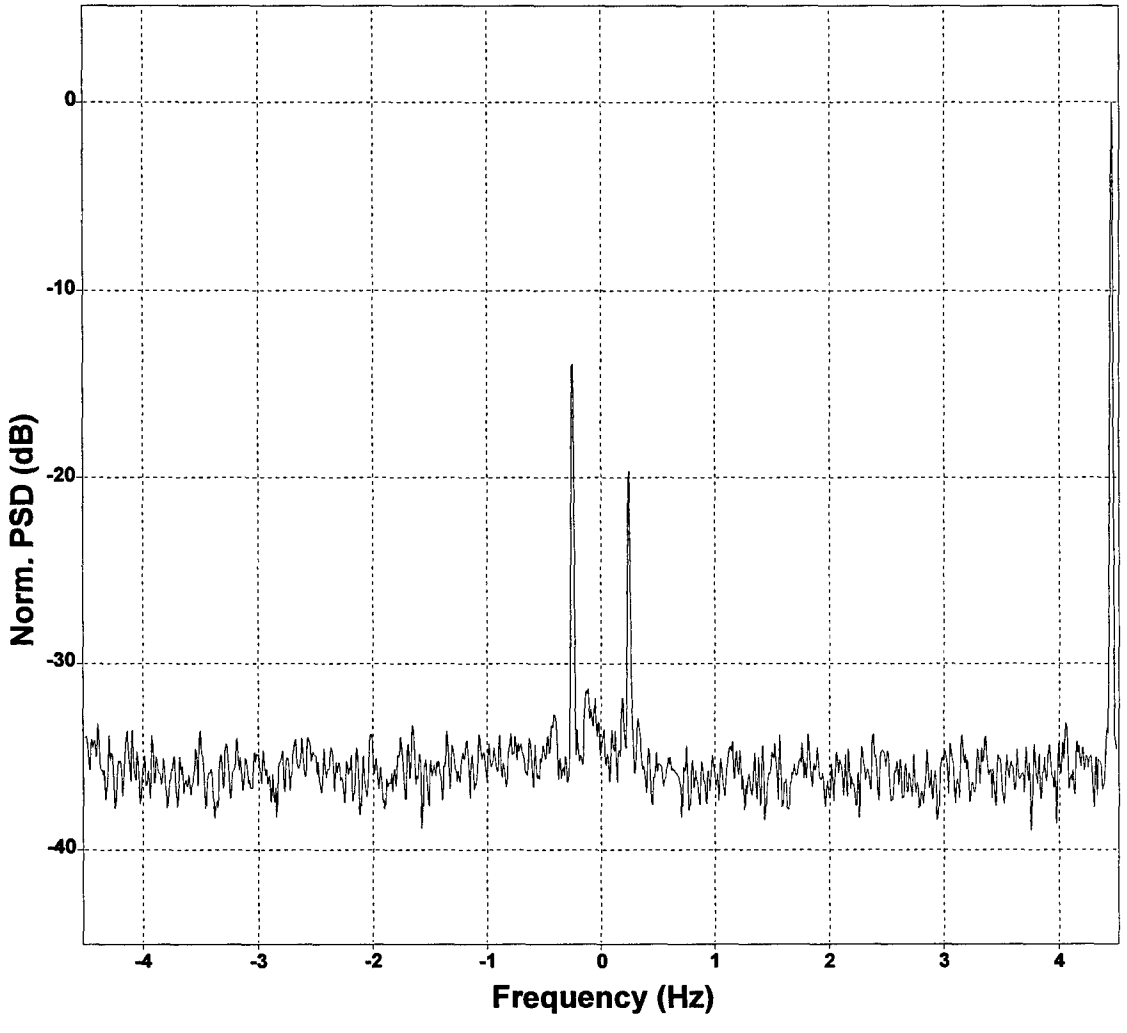

Figure 19 Normalized Power Spectral Density of Output from Adaptive System Using Two Auxiliary Horizontal Dipoles (Antenna Elements 2 and 4, orthogonal & separated); Sliding Window Method was used to Estimate and Update Weight Coefficients

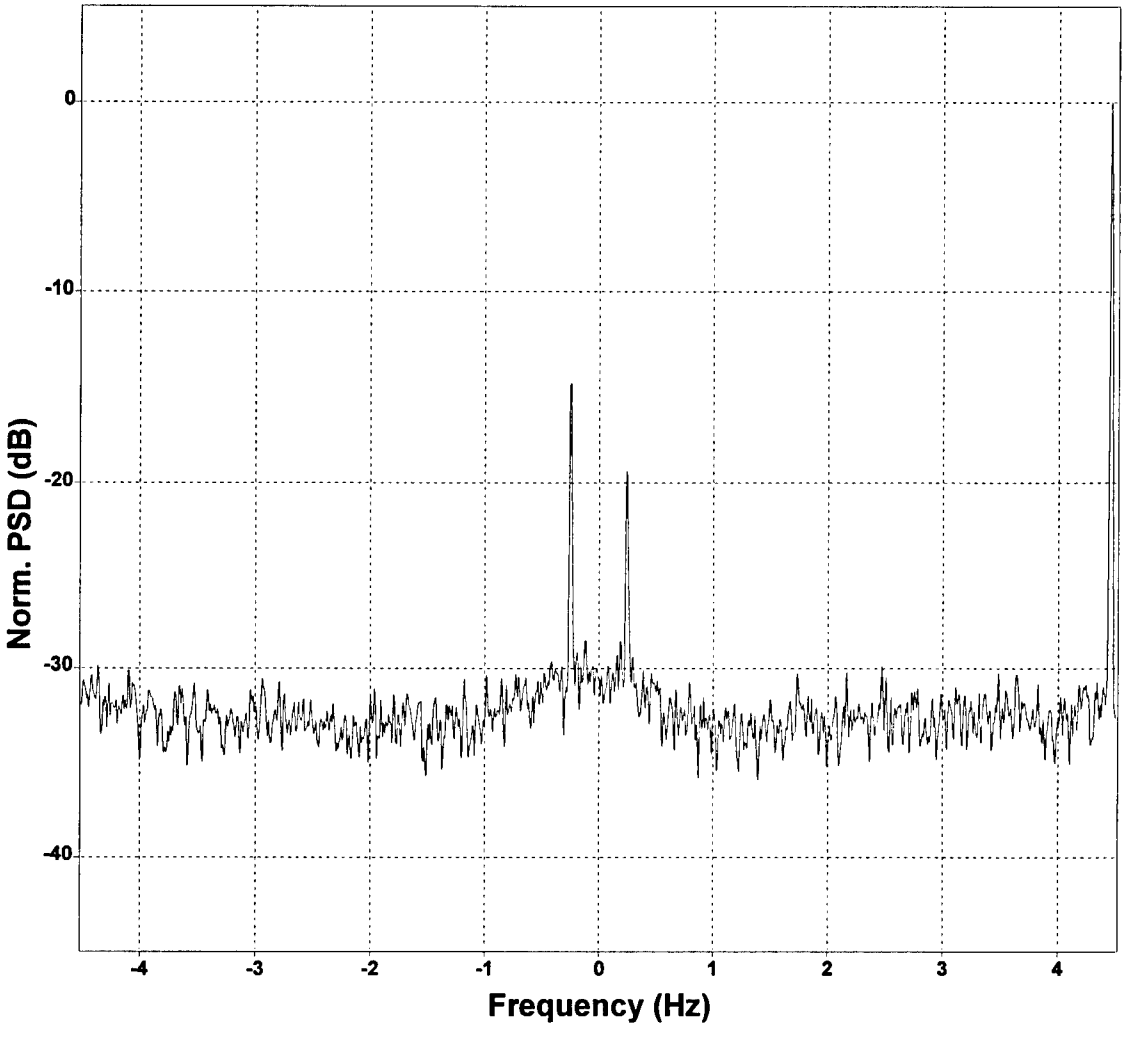

Figure 20 Normalized Power Spectral Density of Output from Adaptive System Using Two Auxiliary Horizontal Dipoles (Antenna Elements 1 and 4, parallel & separated); Sliding Window Method was used to Estimate and Update Weight Coefficients

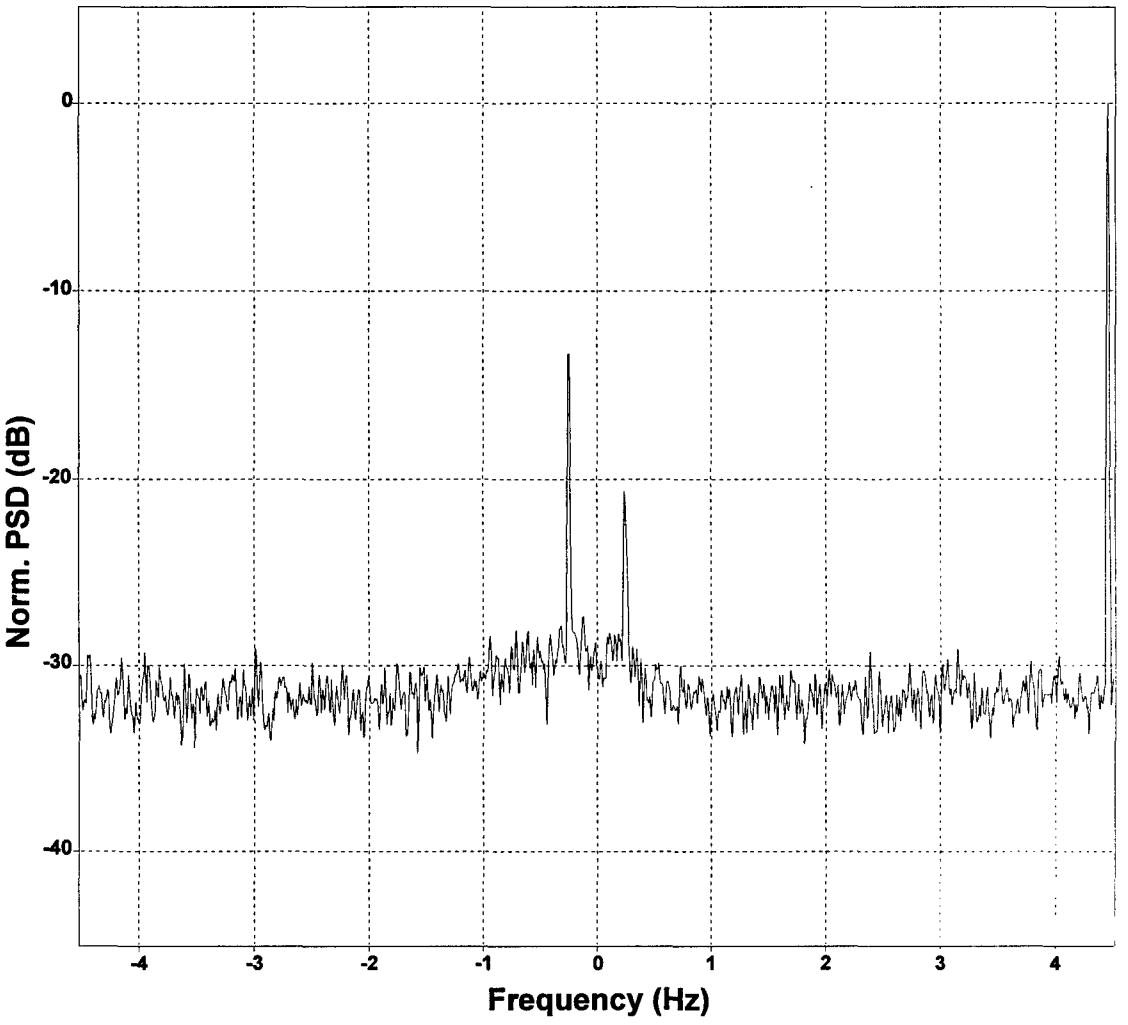

Figure 21 Normalized Power Spectral Density of Output from Adaptive System Using Two Auxiliary Horizontal Dipoles (Antenna Elements 2 and 3, parallel & separated); Sliding Window Method was used to Estimate and Update Weight Coefficients

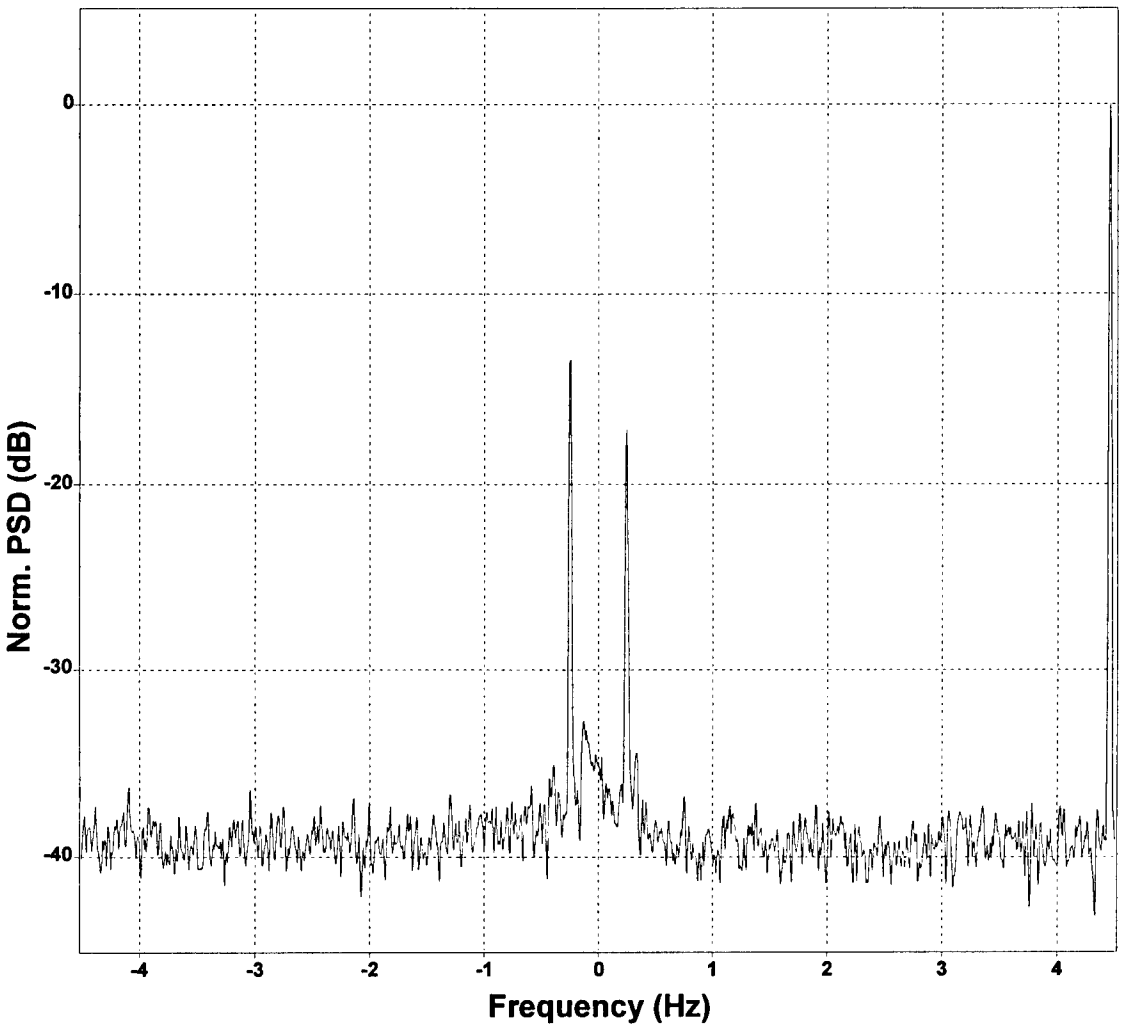

Figure 22 Normalized Power Spectral Density of Output from Adaptive System Using Four Auxiliary Horizontal Dipoles; Sliding Window Method was used to Estimate and Update Weight Coefficients

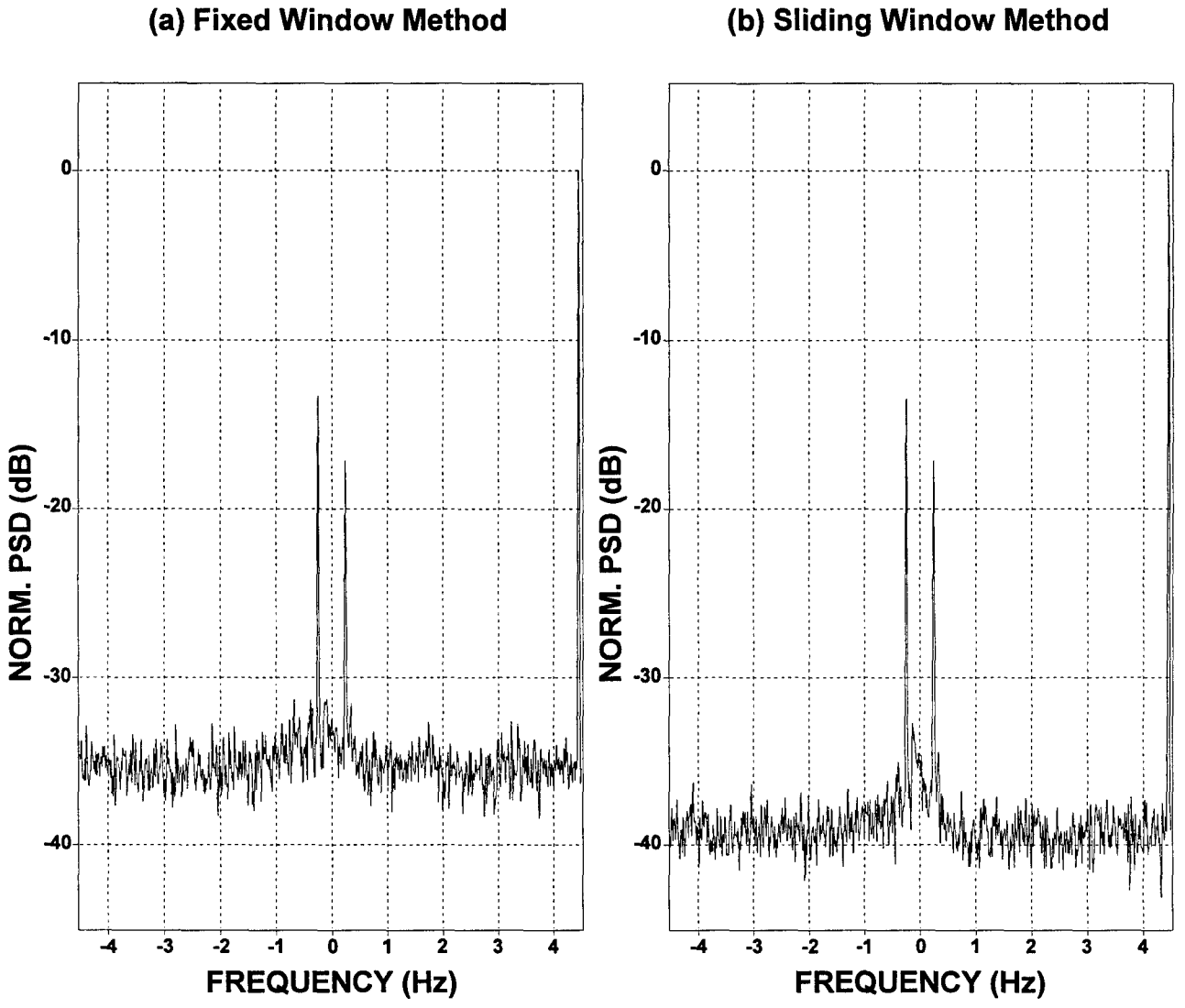

Figure 23 Comparison of PSDs at the Output of Adaptive System Using Fixed Window and Sliding Window Methods; All Four Auxiliary Horizontal Dipoles were used as Auxiliary Antennas

DOCUMENT CONTROL DATA

(Security classification of title, body of abstract and indexing annotation must be entered when the overall document is classified)

1. ORIGINATOR (the name and address of the organization preparing the document. Organizations for whom the document was prepared, e.g. Establishment sponsoring a contractor's report, or tasking agency, are entered in section 8.)

Defence Research Establishment Ottawa

2. SECURITY CLASSIFICATION (overall security classification of the document including special warning terms if applicable)

UNCLASSIFIED

3. TITLE (the complete document title as indicated on the title page. Its classification should be indicated by the appropriate abbreviation (S,C or U) in parentheses after the title.)

Adaptive Suppression of Interference in HF Surface Wave Radar Using Auxiliary Horizontal Dipole Antennas (U)

4. AUTHORS (Last name, first name, middle initial)

Leong, Hank W. H.

5. DATE OF PUBLICATION (month and year of publication of document)	6a. NO. OF PAGES (total containing information. Include Annexes, Appendices, etc.)	6b. NO. OF REFS (total cited in document)
September 1998	65	8

7. DESCRIPTIVE NOTES (the category of the document, e.g. technical report, technical note or memorandum. If appropriate, enter the type of report, e.g. interim, progress, summary, annual, or final. Give the inclusive dates when a specific reporting period is covered.)

DREO Technical Report

8. SPONSORING ACTIVITY (the name of the department project office or laboratory sponsoring the research and development. Include the address.)

DND - Defense Research Establishment Ottawa
Surface Radar Section
Shirley's Bay, Ottawa

9a. PROJECT OR GRANT NO. (If appropriate, the applicable research and development project or grant number under which the document was written. Please specify whether project or grant)	9b. CONTRACT NO. (If appropriate, the applicable number under which the document was written)
05AB11	

10a. ORIGINATOR'S DOCUMENT NUMBER (the official document number by which the document is identified by the originating activity. This number must be unique to this document.)	10b. OTHER DOCUMENT NOS. (Any other numbers which may be assigned this document either by the originator or by the sponsor.)
DREO REPORT 1335	

11. DOCUMENT AVAILABILITY (any limitations on further dissemination of the document, other than those imposed by security classification)

(X) Unlimited distribution
( ) Distribution limited to defence departments and defence contractors; further distribution only as approved
( ) Distribution limited to defence departments and Canadian defence contractors; further distribution only as approved
( ) Distribution limited to government departments and agencies; further distribution only as approved
( ) Distribution limited to defence departments; further distribution only as approved
( ) Other (please specify):

12. DOCUMENT ANNOUNCEMENT (any limitation to the bibliographic announcement of this document. This will normally correspond to the Document Availability (11). However, where further distribution (beyond the audience specified in 11) is possible, a wider announcement audience may be selected.)

UNLIMITED

UNCLASSIFIED

SECURITY CLASSIFICATION OF FORM
(highest classification of Title, Abstract, Keywords)

13. ABSTRACT (a brief and factual summary of the document. It may also appear elsewhere in the body of the document itself. It is highly desirable that the abstract of classified documents be unclassified. Each paragraph of the abstract shall begin with an indication of the security classification of the information in the paragraph (unless the document itself is unclassified) represented as (S), (C), or (U). It is not necessary to include here abstracts in both official languages unless the text is bilingual.)

This report presents the results of a study to evaluate the effectiveness of an adaptive technique using horizontal dipoles to suppress the skywave interference in HF Surface Wave Radar (HFSWR). Four auxiliary horizontal dipole antennas, configured in the form of two separate crosses, were used to form an adaptive system with the vertically polarized antennas (VPA) of a HFSWR system. The outputs of the horizontal dipoles were correlated with the summed output of the VPAs to cancel the interference component in the output of the VPAs. Two slightly different methods were used in the estimation of the correlation coefficients. The first method used the samples at the far ranges of the radar, and the second method used the samples in the range bins close to the range bin selected for the interference suppression. With the first method, the interference-plus-noise power (INP) was reduced by up to 13 dB, and the Bragg-to-interference-plus-noise-ratio (BINR) was increased by up to 21 dB. With the second method, the INP was reduced by up to 17 dB, and the BINR was increased by up to 25 dB. In both methods, we compared the effectiveness of the adaptive technique using one, two or four horizontal dipole antennas. As expected, we found that the technique was the most effective when all the four horizontal dipoles were used.

14. KEYWORDS, DESCRIPTORS or IDENTIFIERS (technically meaningful terms or short phrases that characterize a document and could be helpful in cataloguing the document. They should be selected so that no security classification is required. Identifiers, such as equipment model designation, trade name, military project code name, geographic location may also be included. If possible keywords should be selected from a published thesaurus, e.g. Thesaurus of Engineering and Scientific Terms (TEST) and that thesaurus-identified. If it is not possible to select indexing terms which are unclassified, the classification of each should be indicated as with the title.)

High Frequency (HF)
High Frequency Surface Wave Radar (HFSWR)
Skywave Interference
Interference Suppression
Auxiliary Horizontal Dipole Antenna
Sample Matrix Inversion Method
Fixed Window Method
Sliding Window Method